

VILNIUS UNIVERSITY

Aistė
KADZIAUSKIENĖ

Morphologic Changes of Lamina Cribrosa in Glaucomatous Eyes after Trabeculectomy

SUMMARY OF DOCTORAL DISSERTATION

Medical and Health Sciences
Medicine M 001

VILNIUS 2019

The research was carried out and the dissertation prepared between 2013 and 2019 at Vilnius University.

The research was funded by the Research Council of Lithuania (on the basis of a scholarship granted for academic achievements in 2016).

Academic supervisor

Prof. Dr. Eugenijus Lesinskas [Vilnius University, Medicine and Health Sciences, Medicine M 001]

Academic consultant

Prof. Dr. Leopold Schmetterer [Singapore Eye Research Institute, Duke-NUS Medical School, Lee Kong Chian School of Medicine of Nanyang Technological University, Medical University of Vienna, Medicine and Health Sciences, Medicine M 001]

Members of the Dissertation Defence Panel:

Chair – Prof. Dr. Janina Tutkuvienė [Vilnius University, Medicine and Health Sciences, Medicine M 001].

Members:

Assoc. Prof. Dr. Gerhard Garhöfer [Medical University of Vienna, Medicine and Health Sciences, Medicine M 001],

Prof. Dr. Ingrida Janulevičienė [Lithuanian University of Health Sciences, Medicine and Health Sciences, Medicine M 001],

Prof. Dr. Dalius Jatužis [Vilnius University, Medicine and Health Sciences, Medicine M 001],

Assoc. Prof. Dr. Giedrius Kalesnykas [Tampere University, Medicine and Health Sciences, Medicine M 001].

The dissertation will be defended during a public hearing of the Dissertation Defence Panel on June 7, 2019 at 2:00 p.m. in Room E122 of the Vilnius University Hospital Santaros Klinikos. Address: 2 Santariškių St. Vilnius, Lithuania. Phone No.: +37068556201; email: aistedam@gmail.com.

The text of this dissertation can be accessed at the libraries of Vilnius University as well as on the website of Vilnius University: www.vu.lt/lt/naujienos/ivykiu-kalendorius.

VILNIAUS UNIVERSITETAS

Aistė
KADZIAUSKIENĖ

Akytosios plokštelės morfologiniai pokyčiai po trabekulektomijos glaukoma sergančiųjų akyse

DAKTARO DISERTACIJOS SANTRAUKA

Medicinos ir sveikatos mokslai
Medicina M 001

VILNIUS 2019

Disertacija rengta 2013 – 2019 metais Vilniaus universitete.
Mokslinį darbą rėmė Lietuvos mokslo taryba (2016 m. skirta stipendija už akademinį pasiekimą).

Mokslinis vadovas

prof. dr. Eugenijus Lesinskas [Vilniaus universitetas, medicinos ir sveikatos mokslai, medicina M 001]

Mokslinis konsultantas

prof. dr. Leopold Schmetterer [Singapūro akių tyrimų institutas, Duke-NUS medicinos mokykla, Nanyang technologijos universiteto Lee Kong Chian medicinos mokykla, Vienos medicinos universitetas, medicinos ir sveikatos mokslai, medicina M 001]

Gynimo taryba:

Pirmininkė – prof. dr. Janina Tutkuvienė [Vilniaus universitetas, medicinos ir sveikatos mokslai, medicina M 001].

Nariai:

doc. dr. Gerhard Garhöfer [Vienos medicinos universitetas, medicinos ir sveikatos mokslai, medicina M 001],

prof. dr. Ingrida Janulevičienė [Lietuvos sveikatos mokslų universitetas, medicinos ir sveikatos mokslai, medicina M 001],

prof. dr. Dalius Jatužis [Vilniaus universitetas, medicinos ir sveikatos mokslai, medicina M 001],

doc. dr. Giedrius Kalesnykas [Tampėros universitetas, medicinos ir sveikatos mokslai, medicina M 001].

Disertacija ginama viešame Gynimo tarybos posėdyje 2019 m. birželio 7 d. 14 val. Vilniaus universiteto ligoninės Santaros klinikų Raudonojoje auditorijoje. Adresas: Santariškių g. 2, E122 auditorija, Vilnius, Lietuva, tel. +37068556201, el. paštas aistedam@gmail.com.

Disertaciją galima peržiūrėti Vilniaus universiteto bibliotekoje ir VU interneto svetainėje adresu: <https://www.vu.lt/naujienos/ivykiu-kalendorius>

CONTENT

INTRODUCTION	7
PURPOSE AND OBJECTIVES OF THE RESEARCH.....	9
SCOPE AND METHODOLOGY OF THE RESEARCH	10
Subjects and Study Design	10
Examinations and Measurements	12
Statistical Analysis	17
RESULTS.....	18
Changes in Morphologic Parameters of Lamina Cribrosa	19
Changes in Choroidal and Retinal Thickness.....	24
Factors Associated with Lamina Cribrosa Changes	25
Associations of Lamina Cribrosa Changes with Glaucoma Progression	29
Comparison of Lamina Cribrosa Changes with respect to the Severity and Type of Glaucoma	32
DISCUSSION.....	33
CONCLUSIONS	41
PRACTICAL RECOMMENDATIONS	42
REFERENCES	43
APPROBATION OF THE RESULTS	54
Publications	54
Oral Presentations and Posters	54
CURRICULUM VITAE	56
ACKNOWLEDGEMENT.....	58

ABBREVIATIONS

AL	-	Axial length
BCVA	-	Best corrected visual acuity
BM	-	Bruch's membrane
BMO	-	Bruch's membrane opening
CCT	-	Central corneal thickness
CI	-	Confidence interval
GSI	-	Global shape index
IOP	-	Intraocular pressure
LC	-	Lamina cribrosa
LCD	-	Lamina cribrosa depth
MD	-	Mean deviation
N-T	-	Nasal-temporal
OCT	-	Optical coherence tomography
ONH	-	Optic nerve head
PACG	-	Primary angle-closure glaucoma
PEXG	-	Pseudoexfoliative glaucoma
POAG	-	Primary open-angle glaucoma
PSD	-	Pattern standard deviation
RNFL	-	Retinal nerve fiber layer
S-I	-	Superior-inferior
VF	-	Visual field
VIF	-	Variance inflation factor

INTRODUCTION

Glaucoma is a heterogeneous group of disorders characterized by a cupping of the optic nerve head (ONH) and corresponding visual field defects.¹ It is the leading cause of irreversible blindness worldwide.^{2,3} The global prevalence of glaucoma for people aged 40–80 years is 3.54% (95% CI, 2.09–5.82) and it constantly increases due to the growing and aging population.^{4,5} In 2040, the prevalence of glaucoma worldwide for this age is expected to be 111.8 million.⁴

To date, elevated intraocular pressure (IOP) is proven to be the principal manageable risk factor for the development and progression of glaucoma.^{6–10} However, the exact mechanism of IOP contributing to the glaucomatous injury remains incompletely understood. The lamina cribrosa (LC) is implicated to be the principal site of this damage.^{11–16} IOP is thought to affect the structures of the optic nerve head (ONH) directly as the determinant of the translamellar pressure gradient and indirectly via the induced forces of the sclera.^{17–19} Therefore, the connective tissues of the ONH, including the LC, scleral canal, and peripapillary sclera, constantly bear the biomechanical load, which in certain circumstances results in stress and strain to the tissue.²⁰ The biomechanical paradigm of glaucoma postulates that elevated IOP causes LC compression, stretch, and shear, which lead to lamina deformations, strains on glial cells, and subsequent damage of the retinal ganglion cell axons.^{21,22} LC morphology is related to the onset and progression of glaucoma.^{23–26} Thus, all morphologic parameters describing the biomechanics of LC in relation to IOP are of great importance to provide insights into the fundamental mechanisms of glaucoma pathogenesis and treatment.

For many years, the assessment of the IOP effect on LC was limited to *ex vivo* histomorphometrical studies, experimental animal studies, or theoretical models.^{11,12,27–35} Advanced imaging technologies, such as enhanced depth imaging spectral domain optical coherence tomography (OCT), swept source OCT, and adaptive optics, allowed *in vivo* visualization and quantitative

evaluation of the deep ONH structures.³⁶⁻⁴¹ Since then, the structural and biomechanical characteristics of LC in glaucomatous eyes have been widely investigated. A posterior displacement, thinning, and local defects of the LC have been suggested to occur more often in glaucoma-affected eyes and to be related to the progression of the disease.^{24,26,42-47} A number of studies have reported the anterior or posterior displacement of LC after the IOP change in glaucoma, which depends upon the geometrical and material properties of the ONH connective tissues.^{19,48-56}

So far, the main morphologic parameter in the analysis of the LC and IOP relationship has remained the depth of the LC, which has limitations because of its reference to the plane of Bruch's membrane opening (BMO) and subsequent reliance on the shifting thickness of the choroid.⁵⁷⁻⁶⁰ In this context, the LC parameters describing the LC curvature and shape could play an important role as potential morphologic biomarkers independent of the reference plane. However, data about the IOP effect on the curvature and shape of the LC are limited. Only one study investigated the LC posterior bowing after glaucoma surgery and suggested that an LC curvature index might have value as a parameter relevant to ONH biomechanics.⁶¹ The examined curvature index did not correspond to the actual LC curvature, and the authors referred to the change of the LC configuration as a change in curvature. At present, no research has addressed the global shape of the LC after IOP reduction, and this relationship remains to be determined.

The aim of this prospective observational study was to analyze the long-term changes of the LC shape, curvature, and depth after trabeculectomy. A recently introduced morphologic measure, the global shape index (GSI), was chosen to characterize the geometrical shape of the anterior LC surface as a whole independently from the BMO plane.⁶² Actual LC curvatures were assessed along vertical and horizontal meridians. To our knowledge, this is the first study to assess the response of the overall shape of the LC and its actual curvature to the reduction of IOP in glaucomatous eyes.

PURPOSE AND OBJECTIVES OF THE RESEARCH

Purpose of the Research

To evaluate the morphologic changes of the LC in glaucoma-affected eyes after the IOP reduction following trabeculectomy as well as to assess their relationship to biometric and clinical ocular parameters.

Objectives of the Research

1. To evaluate the long-term changes of the mean and sectoral LC depth, horizontal and vertical curvatures, and global shape after trabeculectomy in glaucomatous eyes.
2. To analyze the relationships of the postoperative LC changes with the possibly associated factors, including IOP, age, biometric ocular parameters, and baseline LC morphology.
3. To assess the associations of the morphologic LC changes after trabeculectomy with the clinical parameters of glaucoma progression.
4. To compare the post-trabeculectomy morphologic LC changes with respect to the type and severity of glaucoma.

SCOPE AND METHODOLOGY OF THE RESEARCH

Subjects and Study Design

A prospective observational study was performed from 2014 to 2017 at Vilnius University Hospital Santaros Klinikos. The approval of the Regional Research Ethics Committee was obtained, and all investigations followed the tenets of the Declaration of Helsinki. Consecutive patients who met the eligibility criteria and signed a written informed consent were enrolled in the study.

The inclusion criteria were as follows: (1) diagnosis of open-angle or primary angle-closure glaucoma; (2) indicated trabeculectomy; (3) best-corrected visual acuity of 0.1 or greater in Snellen decimal scale; (4) refractive error from -6.0 D to +6.0 D of sphere and ± 3.0 D of cylinder. Exclusion criteria were being under 18 years of age, any prior intraocular surgery (except phacoemulsification with intraocular lens implantation), other ophthalmological or neurologic diseases affecting the visual field (VF), and poor image quality of the LC.

Initially, 130 glaucomatous eyes of 124 patients planned for trabeculectomy were enrolled; of these, 12 patients (12 eyes) were excluded because of poor LC visibility (6 eyes), failure to attend more than 2 follow-up visits (3 eyes), failed trabeculectomies (2 eyes), and postoperative complications (1 eye). Finally, we analyzed the data of 112 patients (118 eyes) according to the study protocol (Fig. 1). Ten of these patients missed 1 follow-up visit, and 1 patient missed 2 follow-up visits.

Patients were grouped with respect to the severity of glaucomatous injury into an early-to-moderate glaucoma group (early stage and moderate stage glaucoma) and an advanced glaucoma group (advanced stage glaucoma) as well as with respect to the glaucoma diagnosis – a primary open-angle glaucoma (POAG) group, a primary angle-closure glaucoma (PACG) group, and a pseudoexfoliative glaucoma (PEXG) group.

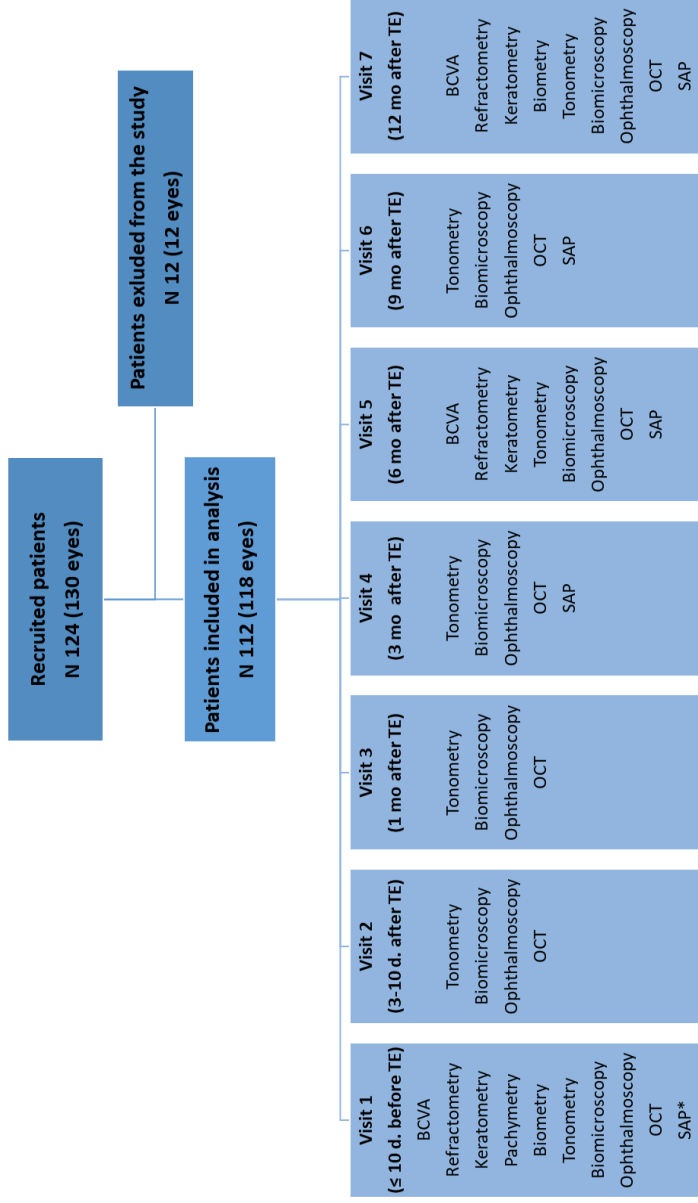


Fig. 1. Study design

BCVA = best corrected visual acuity, OCT = optical coherence tomography, SAP = standard automated perimetry, TE = trabeculectomy.
 * SAP within 1 month before TE.

Examinations and Measurements

Each participant underwent the baseline examination, including an assessment of best-corrected visual acuity using the Snellen chart, an autorefractometry (Topcon KR-1 auto kerato-refractometer Topcon Medical Systems, Tokyo, Japan), an applanation tonometry (Goldmann tonometer, Haag-Streit AG, Koeniz, Switzerland), slit lamp biomicroscopy, a dilated stereoscopic examination of the fundus, a partial optical coherence interferometry (IOL Master, Carl Zeiss Meditec, Dublin, USA), and spectral-domain OCT (Heidelberg Spectralis, Heidelberg Engineering, Dossenheim, Germany). Two baseline VF tests of achromatic automated perimetry using the 30-2 Swedish Interactive Threshold Algorithm Standard strategy (Humphrey visual field analyzer, Carl Zeiss Meditec, Dublin, USA) were performed within 1 month before the trabeculectomy.

Glaucoma diagnosis was based on the presence of glaucomatous optic neuropathy (neuroretinal rim thinning, notching, or retinal nerve fiber layer [RNFL] defects) with or without associated glaucomatous VF defects.⁶³ The stages of glaucoma were defined on the basis of the Hodapp-Parrish-Anderson criteria of standard automated perimetry.⁶⁴

All patients underwent a limbal-based trabeculectomy, with or without adjunctive 5-fluorouracile, following the same surgical protocol by 1 of 4 surgeons. Subsequently, needling with 5-fluorouracile was performed if a failure of the filtering bleb occurred. Only patients with reduced postsurgical IOP continued the study. In all patients a target pressure was defined based on their baseline IOP, their risk factors, and the progression of glaucoma prior to inclusion. Medical treatment was administered during the postoperative period if the target's IOP was exceeded (19.49% of all studied eyes).

We evaluated the morphologic parameters of the LC and IOP within 10 days preoperatively and postoperatively, and at 1, 3, 6, 9, and 12 months postoperatively (Fig. 1). The mean of 2 IOP

measurements was calculated. If 2 measurements differed by more than 2 mmHg, we took a third reading and averaged the 2 closest values. VF tests were repeated at three-month intervals postoperatively. The VF test was considered reliable if false-positive and false-negative errors were less than 33% and fixation losses were less than 20%. Nine patients lacked VF data at the 12-month visit, eighteen patients – at 3-month and 6-month visits, and twenty patients – at the 3-month visit.

Spectral Domain Optical Coherence Tomography

We performed enhanced depth imaging spectral domain OCT to visualize the LC.^{36,39} The ONH was scanned using the Spectralis OCT system by centering a $15^\circ \times 10^\circ$ rectangle scan on the ONH. Each OCT volume consisted of 49 serial horizontal B scans (4.5-mm long lines, 40 images averaged) spaced at approximately 63- μ m intervals.

The RNFL thickness was measured automatically from the circumferential OCT scan of 3.4 mm diameter centered on the ONH (single circle B scan of 12° , 100 images averaged) using Spectralis software (Eye Explorer, Heidelberg Engineering, Germany). The same type of the scan was repeated using the enhanced depth imaging for the visualization of the peripapillary choroid.

We imaged the retina performing a single horizontal linear scan (100 images averaged) and posterior pole scan (61 raster lines spaced 120 μ m apart, 20 images averaged), both centered on the fovea. The subfoveal macular thickness was measured automatically from the single linear scan. The macular map analysis protocol was selected to display numeric averages of the measurements for the central macular subfield (the innermost 1-mm-diameter circle, defined by the Early Treatment Diabetic Retinopathy Study).

At least 2 OCT scans of each type were taken, and the one with the best quality was chosen. Images with a quality score of 15 or less were excluded. The baseline OCT scan was set as a reference, and all subsequent scans done were adherent to it (Spectralis Active Eye

Tracking system). Any potential magnification errors were avoided by entering the corneal curvature and refraction of the eye before the OCT scanning.

Image Delineation, Three-Dimensional Reconstruction, and the Morphologic Measurements of Lamina Cribrosa

We enhanced raw OCT images using adaptive compensation (Reflectivity software, version 3.4, Ophthalmic Engineering & Innovation Laboratory, National University of Singapore, Singapore). Such post-processing has been shown to remove shadows, enhance tissue contrast, and improve the visibility of the LC.⁶⁵⁻⁶⁷ Afterward, 2 ophthalmologists delineated and reconstructed the ONH volumes using semi-automated software Morphology 1.0 (version 1.0, Ophthalmic Engineering & Innovation Laboratory, National University of Singapore, Singapore). The anterior border of the LC was defined and manually marked on each B-scan as the upper margin of hyper-reflective tissue below the ONH tissues, extending laterally up to the LC insertions to the sclera (Fig. 2). The regions with an undistinguishable LC border were not delineated. The Morphology 1.0 software determined the border of the LC area as the contour of all delineated points. On average, there were 259 (median 258, range 148–433) marked points per ONH scan included in the analysis. We also defined and delineated the BMO as the end points of hyper-reflective Bruch’s membrane layer on either side of the ONH in each B-scan.

Subsequently, the Morphology 1.0 software 3D reconstructed the LC anterior surface and BMO plane and automatically calculated the BMA area and LC morphologic parameters according to the earlier established protocols as follows.^{62,68} The average LC visibility (LC coverage of BMO area evaluated by the software and expressed in %) of 130 enrolled eyes was 89.8% (median 94.2, range 29.8–97.8). Finally, 118 ONH with LC visibility of greater than 70% (mean 92.4, median 95.1, range 71.3-97.8) were analyzed.

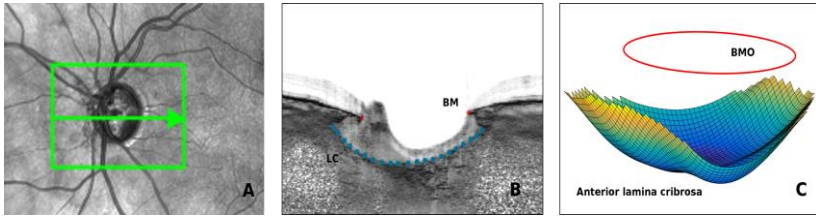


Fig. 2. The imaging, delineation, and reconstruction of the lamina cribrosa (LC). We scanned the optic nerve head (ONH) by serial horizontal B scans spaced at approximately 63- μ m intervals using enhanced depth imaging OCT. (A) Infrared image of the ONH demonstrates the place of the horizontal section where the B scan was located. (B) A cross-sectional view of the ONH after the adaptive compensation (Reflectivity software) and delineation of the anterior LC and the end points of Bruch's membrane (BM) using Morphology 1.0 software. (C) A three-dimensional view of the reconstructed LC and plane of the Bruch's membrane opening (BMO).

Lamina Cribrosa Depth (LCD). The software measured the LCD as the distance between the BMO plane and the anterior surface of the LC, which was reconstructed from the delineated LC points.⁶⁸ The mean LCD was calculated as the mean depth of all points on the LC surface. The lamina was automatically divided with respect to the center of the BMO ellipse into six sectors, comprising four 45° sectors (superotemporal, superonasal, inferotemporal, and inferonasal) and two 90° sectors (temporal and nasal). The sectoral LCD were assessed.

Lamina Cribrosa Curvature. The LC curvature was measured automatically in two principal meridians: superior-inferior (S-I) and nasal-temporal (N-T). Morphology 1.0 first intersects the anterior LC surface with 180 radial cross-sections that pass through the center of the BMO ellipse perpendicularly to it. An LC curve for each cross-section is generated.⁶² Then, a circular arc is fitted to the LC curves along S-I and N-T directions. This approach enables estimation of LC curvatures along different radial orientations in a global sense without compromising robustness.⁶² We expressed the values in

mm,¹ with negative values describing a posteriorly curved LC and positive values indicating an anteriorly curved LC.

Lamina Cribrosa Global Shape Index. The LC GSI assessment was based on global curvature measurements along radial LC directions and defined as:

$$\text{LC GSI} = (2/\pi) \tan^{-1} ((\kappa_1 + \kappa_2)/(\kappa_1 - \kappa_2)); (\kappa_1 \geq \kappa_2).$$

where κ_1 and κ_2 are maximum and minimum principal arc curvatures of LC, respectively.⁶² The value of the LC GSI varies between -1 and 1 and corresponds to a transition from a spherical cup (posteriorly curved LC; GSI = -1) through a symmetric saddle-shaped LC (GSI = 0) to a spherical cap (anteriorly curved LC; GSI = 1). Fig. 3 demonstrates the scale of LC GSI with the corresponding LC shapes. This index has previously been validated as an LC global shape parameter by Thakku et al.⁶²

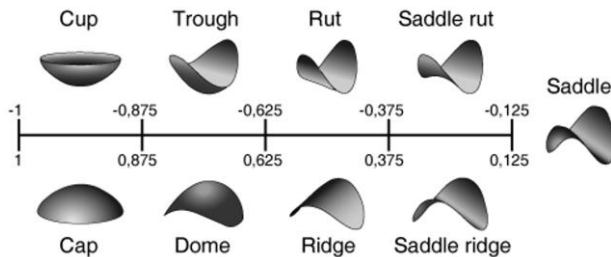


Fig. 3. A global shape index scale of the lamina cribrosa representing 9 intervals with corresponding shapes. Modified from Thakku et al.⁶²

Measurements of the Peripapillary Choroid

The peripapillary choroidal thickness was measured manually from the circumferential enhanced depth imaging OCT scan 1.7 mm superiorly, temporally, inferiorly, and nasally to the center of the ONH with a caliper of Spectralis software. The choroidal thickness was defined as the distance from the hyper-reflective outer border of the retinal pigment epithelium to the hypo-reflective subchoroidal space or choroidal-scleral interface. The mean peripapillary

choroidal thickness from the measurements at four listed locations was calculated.

Statistical Analysis

We analyzed the data using R statistical software. The study sample was calculated using the G*Power statistical package.⁶⁹ Continuous variables were described by mean and standard deviation (SD). We used the Friedman rank sum test and the Nemenyi post-hoc test to compare the preoperative and postoperative measurements. The quantitative parameters of independent samples were compared using the Kruskal-Wallis test and the Two-sample Wilcoxon test, while the qualitative parameters – using the Chi-Square test. The significance test for the Pearson correlation coefficient was used to evaluate the correlation in between the changes of morphologic LC parameters at each time point. We performed a linear mixed model analysis for longitudinal data to evaluate the associations between the changes of LC morphology with possible explanatory variables. In addition to age and sex, variables with $P < 0.1$ from the univariate models were included in the multivariate model. We used generalized estimating equation models to evaluate the relationship between the clinical parameters of glaucoma progression with the postoperative LC changes. A P value of < 0.05 was considered statistically significant.

The reproducibility of the LC measurements was determined on the basis of the LC GSI and LCD evaluation in 20 ONH scans and showed good intergrader (intraclass correlation coefficient (ICC) 0.948, 95% confidence interval (CI): 0.875-0.979; ICC 0.991, 95%CI: 0.977-0.996, respectively) and intragrader (ICC 0.986, 95%CI: 0.966-0.994; ICC 0.999, 95%CI: 0.998-1.0, respectively) agreements.

RESULTS

In total, we analyzed the data of 118 eyes (112 patients). The demographic and clinical baseline characteristics of the patients are presented in Table 1. The mean (\pm SD) age of the patients was 67.6 ± 8.8 years and 52% were female. More than half of the patients had an advanced stage of glaucoma – 79 (66.95%), with PEXG being the most common diagnosis in the study sample – 89 (75.42%).

The mean IOP was reduced at all follow-up visits ($P < 0.001$) (Fig. 4, Table 2). At the first follow-up, the IOP reduction was the greatest when compared with later visits ($P < 0.001$); it stabilized after the first postoperative month ($P > 0.05$ in between the subsequent visits).

Table 1. Patient demographic and clinical characteristics.

Baseline characteristic	Value
Age, years	67.6 ± 8.8
Male/female	54/58
BCVA*	0.67 ± 0.25
Refractive error, D	-0.4 ± 2.0
Central corneal thickness, μm	520 ± 33
Axial eye length, mm	23.63 ± 0.92
Visual field MD, dB	-14.69 ± 8.91
Global RNFL thickness, μm	53.73 ± 14.01
Glaucoma type, % (eyes)	
Pseudoexfoliative	75.42 (89)
Primary open-angle	17.8 (21)
Primary angle-closure	6.78 (8)
Glaucoma severity, % (eyes)	
Mild-to-moderate	33.05 (39)
Mild	16.95 (20)
Moderate	16.1 (19)
Advanced	66.95 (79)

*BCVA = best corrected visual acuity; D = diopters; MD = mean deviation; RNFL = retinal nerve fiber layer. Values expressed as mean \pm SD unless otherwise indicated. * - decimal notation.*

Table 2. Intraocular pressure before and after glaucoma surgery.

	Baseline	Postoperative					
		3-10 days	1 month	3 months	6 months	9 months	12 months
IOP, mmHg	27.6 ± 6.7	9.2 ±3.9	12.8 ±4.2	12.6 ±3.4	12.6 ±3.2	13.2 ±3.4	13.5 ±3.7
IOP reduction,* mmHg	-	18.3 ±7.7	15.0 ±7.4	15.1 ±7.3	15.1 ±7.5	14.5 ±7.3	14.3 ±7.7
IOP reduction,* %	-	65.0 ±16.9	51.9 ±17.3	52.2 ±16.1	52.0 ±16.4	49.8 ±17.5	48.5 ±18.8

*IOP = intraocular pressure. The values are expressed as mean ± SD. * IOP reduction from baseline, $P < 0.001$ at all follow-up visits (pairwise comparisons of the Nemenyi multiple comparison test).*

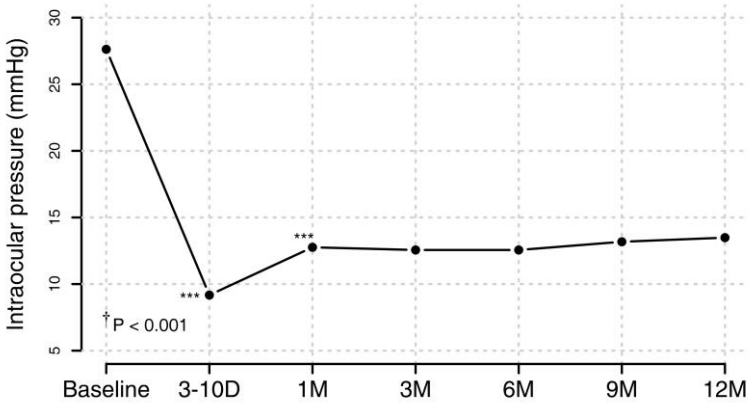


Fig. 4. A line graph showing the dynamics of intraocular pressure during the follow-up. The mean IOP reduced at all follow-up visits compared to baseline ($P < 0.001$). † P value of the Friedman rank sum test. * P values for comparison with the previous follow-up visit obtained using the Nemenyi multiple comparison test, *** $P \leq 0.001$.

Changes in Morphologic Parameters of Lamina Cribrosa

Lamina Cribrosa Depth

The mean and sectoral LCD decreased (shallowed) at all follow-up visits after the trabeculectomy ($P < 0.001$) (Fig. 5, Table 3). After the mean LCD decreased until the sixth month, there were no significant changes in between the later visits ($P > 0.05$). The trend

of temporal sequence of LCD seemed to be consistent for all LCD parameters (Fig. 5).

Before the trabeculectomy, the superonasal sector of the LC was the deepest and the temporal sector was the shallowest when compared with the others ($P < 0.001$). During the early postoperative period, the LCD decreased more significantly in both superior sectors when compared with the inferior, nasal, and temporal ones ($P \leq 0.02$). After a year, the superonasal LCD showed the greatest decrease compared with other sectors ($P \leq 0.001$), except the superotemporal sector ($P = 0.21$); the LCD change was the least in the temporal sector when compared with others ($P \leq 0.006$).

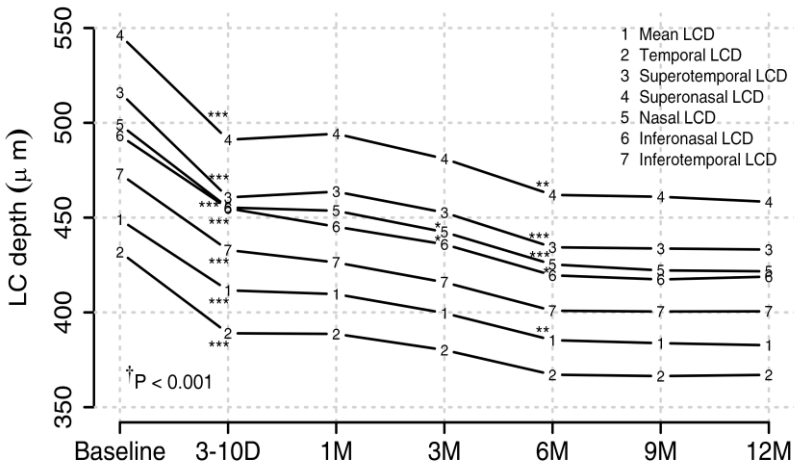


Fig. 5. A line graph demonstrating the time course of mean and sectoral lamina cribrosa (LC) depth after trabeculectomy. All LC depth (LCD) parameters decreased from baseline at all postoperative follow-ups ($P < 0.001$). The mean and sectoral LCD, except the temporal and inferotemporal, were deeper at 1 week, 1 month, and 3 months when compared with 6, 9, and 12 months postoperatively ($P \leq 0.02$). There were no changes in between the visits after 6 months. † P values of the Friedman rank-sum test for all LCD parameters. * P values for comparison with the previous follow-up visit obtained using the Nemenyi multiple comparison test, * $P \leq 0.05$; ** $P \leq 0.01$; *** $P \leq 0.001$.

Table 3. Shape, curvature, and depth parameters of the lamina cribrosa during the post-trabeculectomy year.

Parameter	Baseline				Postoperative				P* value
	3-10 days	1 month	3 months	6 months	9 months	12 months	12 months	12 months	
N-T curvature, mm ⁻¹	-617 ±191	-566 ±186	-547 ±167	-527 ±162	-531 ±167	-526 ±163	-526 ±163	-526 ±163	<0.001
S-I curvature, mm ⁻¹	-334 ±655	-238 ±512	-199 ±455	-191 ±471	-183 ±417	-156 ±419	-156 ±419	-156 ±419	0.006
Global shape index	-0.622 ±0.18	-0.613 ±0.19	-0.611 ±0.19	-0.617 ±0.18	-0.617 ±0.18	-0.605 ±0.19	-0.605 ±0.19	-0.605 ±0.19	0.03
Mean LCD, µm	449 ±129	410 ±108	400 ±104	385 ±100	384 ±100	383 ±101	383 ±101	383 ±101	<0.001
Sectoral LCD, µm									
Temporal	432 ±146	389 ±119	380 ±113	367 ±108	366 ±109	367 ±109	367 ±109	367 ±109	<0.001
Superotemporal	516 ±171	464 ±138	453 ±132	434 ±126	434 ±128	433 ±127	433 ±127	433 ±127	<0.001
Superonasal	546 ±173	494 ±140	481 ±134	462 ±129	461 ±131	458 ±128	458 ±128	458 ±128	<0.001
Nasal	499 ±153	454 ±124	442 ±119	425 ±113	422 ±114	422 ±115	422 ±115	422 ±115	<0.001
Inferonasal	493 ±153	445 ±137	436 ±125	420 ±119	417 ±119	419 ±122	419 ±122	419 ±122	<0.001
Inferotemporal	473 ±153	426 ±127	416 ±123	401 ±117	400 ±117	401 ±119	401 ±119	401 ±119	<0.001

LCD = lamina cribrosa depth, N-T = nasal-temporal, S-I = superior-inferior. The values are expressed as mean ± standard deviation. The values are expressed as mean ± SD. * P values were obtained with the Friedman rank-sum test.

The postoperative LCD decreased from the baseline (shallowing of the LC) in the majority of the cases. However, 28 patients (35 visits) showed an increase in their LCD from the baseline (deepening of the LC) in at least one visit during the follow-up period. Most of those with an increase in the LCD were observed during the first postoperative month and reduced significantly over time (P for trend < 0.001) (Table 4). In the group with a decreased postoperative LCD, the patients tended to be younger (66.4 ± 8.1 y, $P = 0.002$) and have thinner baseline RNFL (51.9 ± 12.6 μm , $P = 0.04$) compared with those eyes with an increased postoperative LCD (71.2 ± 9.3 y, 59.7 ± 16.7 μm , respectively). There were no significant differences in terms of their gender, baseline IOP, IOP reduction, axial length, VF MD, or baseline LC parameters between the eyes with decreased and increased postoperative LCD ($P > 0.05$). IOP reduction was related to a greater LCD change in both groups. However, the effect was greater in the eyes in which the LC became shallower ($\beta = 1.67$; 95% CI, 1.1 – 2.24; $P < 0.001$) than in those eyes in which the LCD became deeper ($\beta = 0.84$; 95% CI, 0.31 – 1.36; $P = 0.002$) after the surgery. In other words, eyes with shallower LCD compared with baseline responded to IOP reduction with greater movement anteriorly than eyes with deeper LCD ($P = 0.002$).

Table 4. The proportions of eyes according to the change of lamina cribrosa depth during follow-up.

Number of eyes N (%)	Postoperatively					
	3-10 days	1 month	3 months	6 months	9 months	12 months
LCD decrease	107 (92.2)	103 (89.6)	112 (94.9)	110 (95.7)	116 (99.1)	114 (98.3)
LCD increase*	9 (7.8)	12 (10.4)	6 (5.1)	5 (4.3)	1 (0.9)	2 (1.7)

*LCD = lamina cribrosa depth. * The number of eyes with LCD increase reduced over time (P for trend < 0.001 , Cochran-Armitage test for trend).*

Lamina Cribrosa Curvature

There was a flattening of both N-T and S-I curvatures of the LC after the trabeculectomy ($P < 0.001$, $P = 0.006$, respectively) (Fig. 6, Table 3). The N-T curvature flattened from baseline at all follow-up visits ($P < 0.001$). It was more curved at the first month when compared with the curvature at 6, 9, and 12 months after surgery ($P \leq 0.02$) and at the 3rd month when compared to 12 months ($P = 0.03$). There were no changes in between the visits after the 6th month ($P > 0.05$). The flattening of S-I curvature was significant at 1 week and 12 months postoperatively ($P = 0.001$, $P = 0.003$, respectively); no changes were found in between other follow-ups.

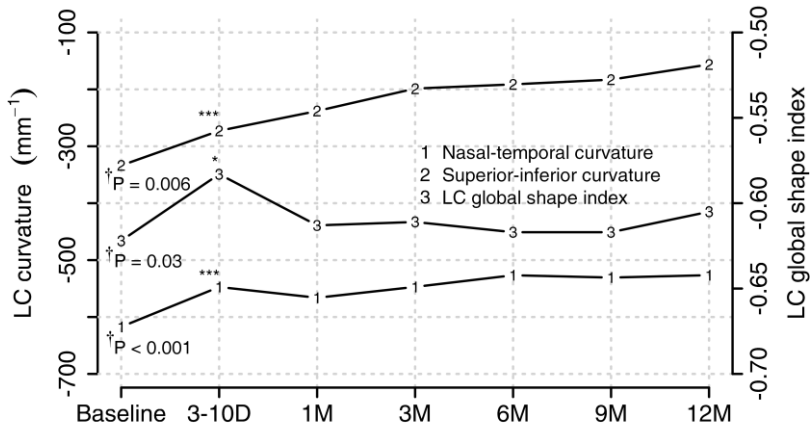


Fig. 6. A line graph showing the time course of the lamina cribrosa (LC) shape index and curvatures after trabeculectomy.

The N-T curvature flattened from the baseline at all follow-up visits ($P < 0.001$); a flattening of the S-I curvature was significant only at the first and last postoperative visits ($P_1 = 0.001$, $P_2 = 0.003$, respectively). The GSI increased from the baseline to the first follow-up ($P = 0.02$) and then decreased from the first follow-up to 3, 6, and 9 months ($P_1 = 0.04$, $P_2 = 0.049$, $P_3 = 0.02$, respectively). † P values of the Friedman rank-sum test. * P values for comparison with the previous follow-up obtained using the Nemenyi multiple comparison test, * $P \leq 0.05$; ** $P \leq 0.01$; *** $P \leq 0.001$.

Lamina Cribrosa Shape

The mean GSI changed from the baseline only in the early postoperative period ($P = 0.02$) when the IOP reduction was the greatest (Figure 6, Table 3). Its positive shift represented a change toward the saddle-shaped LC (less concave N-T meridian and closer to flat or anteriorly curved S-I axis). There were no statistically significant differences in the frequencies of LC GSI intervals between the visits ($P > 0.05$).

Changes in Choroidal and Retinal Thickness

The peripapillary choroidal thickness and retinal thickness at the macular central subfield decreased at all follow-up visits after the trabeculectomy ($P_1 < 0.001$, $P_2 \leq 0.007$, respectively), meanwhile the foveal retinal thickness did not change significantly (Table 5). A significant thinning of the mean RNFL compared to the baseline was observed from the 3rd to 12th months of the follow-up ($P < 0.001$) (Table 5).

Table 5. The dynamics of choroidal and retinal thickness during the follow-ups.

Parameter	Thickness of the parameter (μm)						
	Baseline	Postoperative					
		3-10 days	1 month	3 months	6 months	9 months	12 months
RNFL	53.73 ± 14.01	54.27 ± 14.28	52.44 ± 14.05	51.40 $\pm 13.57^{***}$	50.96 $\pm 13.59^{***}$	50.11 $\pm 13.28^{***}$	49.68 $\pm 12.86^{***}$
Macular central subfield	266 ± 18	270 $\pm 18^{**}$	267 $\pm 18^{**}$	268 $\pm 18^{**}$	269 $\pm 19^{**}$	267 $\pm 18^{**}$	267 $\pm 19^{**}$
Fovea	226 ± 16	228 ± 19	225 ± 16	226 ± 16	226 ± 17	225 ± 16	225 ± 17
Peripapillary choroid	120 ± 51	153 $\pm 61^{***}$	138 $\pm 57^{***}$	135 $\pm 55^{***}$	131 $\pm 56^{***}$	131 $\pm 56^{***}$	130 $\pm 56^{***}$

*RNFL = retinal nerve fiber layer. The values are expressed as mean \pm SD. $^{***} P < 0.001$; $^{**} P < 0.01$, P values for comparison with baseline (Nemenyi multiple comparison test).*

Factors Associated with Lamina Cribrosa Changes

Lamina Cribrosa Depth

After trabeculectomy, a greater decrease of the mean LCD was associated with a younger age, greater IOP reduction, more anteriorly-posteriorly and nasally-temporally curved preoperative LC, and greater baseline GSI (Table 6). The association of the decrease of the mean LCD with a lower baseline IOP was nearly significant ($\beta = -1.89 \mu\text{m}/\text{mmHg}$, 95% CI, -3.84 to 0.05, $P = 0.059$). To avoid multicollinearity, the effect of the axial length shortening on the LCD changes was analyzed in a separate multivariate model from the IOP reduction. The axial length shortening remained associated with the LC shallowing $\beta = 106.62 \mu\text{m}/\text{mm}$; 95% CI, 37.52 – 175.72; $P = 0.003$) (VIF < 2).

The sectoral associations were also tested. The greater decrease in the inferotemporal, superotemporal, and superonasal LCD were related to the thinner corresponding regional baseline RNFL (inferotemporal: $\beta = -0.43 \mu\text{m} / \mu\text{m}$; 95% CI, -0.82 – 0.03; $P = 0.038$; superotemporal: $\beta = -0.67 \mu\text{m} / \mu\text{m}$; 95% CI, -1.32 – -0.01; $P = 0.049$; superonasal: $\beta = -0.84 \mu\text{m}/\mu\text{m}$; 95% CI, -1.65 – -0.03; $P = 0.045$). However, these relationships became insignificant after adjusting for age and gender.

There was no association of the LCD change neither with retinal nor choroidal thickness (at baseline or postoperative change) after adjusting for age and gender ($P > 0.05$).

Table 6. A regression analysis of the factors associated with the postoperative changes of the mean lamina cribrosa depth.

Variable	Change of mean LC depth		P
	Univariate β (95% CI)	Multivariate β (95% CI)	
Age, year	-2.76 (-3.88 to -1.65)	-2.27 (-3.05 to -1.50)	<0.001
Male sex	-6.17 (-26.32 to 13.98)	-9.81 (-22.1 to 2.48)	0.550
AL preoperative, mm	3.40 (-8.01 to 14.80)		0.561
IOP preoperative, mmHg	2.11 (0.67 to -3.55)		0.005
IOP reduction,* mmHg	2.55 (1.33 to 3.77)		<0.001
CCT preoperative, μm	-0.15 (-0.45 to 0.16)	-1.89 (-3.84 to 0.05)	0.350
VF MD preoperative, dB	-0.82 (-1.94 to 0.30)	2.78 (1.07 to 4.49)	0.156
VF MD decrease,* dB	-1.62 (-6.38 to 3.14)		0.506
RNFL preoperative, μm	-0.81 (-1.54 to -0.09)	-0.0003 (-0.48 to 0.48)	0.030
RNFL thinning,* μm	1.20 (-1.21 to 3.61)		0.330
BMO preoperative, μm^2	-27.37 (-52.76 to -1.98)	6.10 (-11.23 to 23.43)	0.037
GSI preoperative, μm	-55.27 (-109.57 to -0.97)	52.29 (12.72 to 91.86)	0.049
N-T curvature preoperative, mm^{-1}	-0.15 (-0.20 to -0.11)	-0.08 (-0.11 to -0.04)	<0.001
S-I curvature preoperative, mm^{-1}	-0.06 (-0.07 to -0.04)	-0.05 (-0.06 to -0.03)	<0.001

AL = axial length; BMO = Bruch's membrane opening; CI = confidence interval; CCT = central corneal thickness; GSI = global shape index; IOP = intraocular pressure; LC = lamina cribrosa; MD = mean deviation; N-T = nasal-temporal; RNFL = retinal nerve fiber layer; S-I = superior-inferior; VF = visual field. * Change at the 12th month of follow-up.

Lamina Cribrosa Curvature

A multivariate regression analysis showed an association between the flattening of the N-T curvature with younger age, lower baseline IOP, greater IOP reduction, and RNFL thinning over a year (Table 7). The postoperative flattening of S-I curvature was associated with more negative baseline GSI, deeper baseline LC, and flatter baseline N-T curvature (Table 7). To avoid multicollinearity, the effect of axial length shortening on the changes of the N-T curvature was analyzed in a separate model from the IOP reduction. The axial length shortening stayed significantly associated with the LC flattening ($\beta = -272.08 \text{ mm}^{-1}/\text{mm}$; 95% CI, $-401.95 - -142.21$; $P < 0.001$; VIF < 2).

Postoperatively, there was a positive relation of the N-T flattening with the greater thickening of the peripapillary choroid ($\beta = 0.9 \text{ mm}^{-1}/\mu\text{m}$; 95% CI, $0.54 - 1.27$; $P < 0.001$) and central macular subfield ($\beta = 1.51 \text{ mm}^{-1}/\mu\text{m}$; 95% CI, $0.68 - 2.34$; $P = 0.003$) after adjusting for age and gender. No association of the S-I flattening with the retinal and choroidal thickness (at the baseline or change) was found ($P > 0.05$).

Lamina Cribrosa Shape

The postoperative GSI change toward a positive value (the direction of cap) was associated with the more superiorly-inferiorly curved preoperative LC, RNFL thinning over a year, and IOP reduction (after adjusting for age, gender, and baseline RNFL thickness) (Table 8).

Postoperatively, there was a positive relation of the GSI increase with a greater thickening of the peripapillary choroid ($\beta = 0.001 /\mu\text{m}$; 95% CI, $0.006 - 0.01$; $P < 0.001$) and central macular subfield ($\beta = 0.003 /\mu\text{m}$; 95% CI, $0.003 - 0.001$; $P = 0.005$) after the adjustment for age and gender. No association with the baseline choroidal or retinal parameters was found.

Table 7. A regression analysis of factors associated with the postoperative changes of the lamina cribrosa curvature.

Variable	Change of N-T curvature			Change of S-I curvature		
	Univariate		Multivariate	Univariate		Multivariate
	β (95% CI)	P	β (95% CI)	P	β (95% CI)	P
Age, year	3.50 (1.91 to 5.09)	<0.001	3.23 (1.75 to 4.71)	<0.001	6.06 (-4.53 to 16.64)	0.265
Male sex	-3.51 (-31.69 to 24.67)	0.808	1.24 (-22.12 to 24.60)	0.917	1.29 (-173.08 to 175.66)	0.988
AL preoperative, mm	-3.47 (-19.41 to 12.47)	0.671			-43.82 (-142.17 to 54.52)	0.384
IOP preoperative, mmHg	-3.01 (-5.02 to -1.00)	0.004	4.26 (0.49 to 8.03)	0.029	-13.99 (-26.63 to -1.35)	0.032
IOP reduction, * mmHg	-3.59 (-5.30 to -1.89)	<0.001	-5.92 (-9.14 to -2.67)	<0.001	-14.69 (-25.69 to -3.68)	0.010
CCT preoperative, μm	0.14 (-0.29 to 0.56)	0.534			0.15 (-2.51 to 2.80)	0.915
VF MD preoperative, dB	1.16 (-0.40 to 2.73)	0.148			3.94 (-5.80 to 13.68)	0.429
VF MD decrease, * dB	5.49 (-1.27 to 12.25)	0.115			10.86 (-29.57 to 51.28)	0.600
RNFL preoperative, μm	1.09 (0.07 to 2.10)	0.038	0.85 (-0.14 to 1.84)	0.905	3.67 (-2.68 to 10.03)	0.260
RNFL thinning, * μm	-3.93 (-7.23 to -0.63)	0.021	-4.22 (-7.59 to -0.85)	0.016	6.86 (-13.99 to 27.71)	0.520
BMO preoperative, μm^2	36.49 (0.98 to 72.01)	0.047	22.21 (-8.82 to 53.23)	0.164	221.36 (1.51 to 441.21)	0.051
LCD preoperative, μm	-0.13 (-0.24 to -0.02)	0.017	-0.01 (-0.11 to 0.08)	0.774	-1.85 (-2.44 to -1.27)	< 0.001
GSI preoperative	24.57 (-52.51 to 101.64)	0.533			814.46 (362.19 to 1266.72)	< 0.001
N-T curvature preoperative, mm^{-1}	-	-			0.68 (0.24 to 1.12)	0.003
S-I curvature preoperative, mm^{-1}	0.02 (-0.01 to 0.04)	0.135			-	-

AL = axial length; BMO = Bruch's membrane opening; CCT = central corneal thickness; CI = confidence interval; GSI = global shape index; IOP = intraocular pressure LC = lamina cribrosa; LCD = lamina cribrosa depth; MD = mean deviation; N-T = nasal-temporal; RNFL = retinal nerve fiber layer; S-I = superior-inferior; VF = visual field. * Change at the 12th month of follow-up.

Interrelations of Morphologic Lamina Cribrosa Changes

The magnitude of the changes in GSI correlated with flattening of the S-I curvature ($\rho_1 = 0.517$, $\rho_2 = 0.724$, $P < 0.001$) and shallowing of the mean LCD ($\rho_1 = 0.363$, $\rho_2 = 0.231$, $P < 0.05$) at the first and last visits, respectively. The correlation of change in GSI with the changes in the N-I curvature was significant only in the early postoperative period ($\rho = 0.351$, $P < 0.001$). There was a positive correlation between the flattening of both LC curvatures and the shallowing of LC during the entire follow-up period ($\rho_1 = 0.647$, $\rho_2 = 0.515$, $P < 0.001$, N-T and S-I curvatures after 12 months, respectively). The flattening of the LC at both principal meridians correlated between each other ($\rho_1 = 0.258$, $P_1 = 0.005$; $\rho_2 = 0.232$, $P_2 = 0.012$ the first and the last follow-ups, respectively).

Associations of Lamina Cribrosa Changes with Glaucoma Progression

A GEE model analysis revealed that a greater RNFL thinning during a year after trabeculectomy was related to a greater postoperative LC shallowing ($\beta = 0.016 \mu\text{m}/\mu\text{m}$, 95% CI, 0.01-0.02, $P < 0.001$), N-T flattening ($\beta = 0.005 \mu\text{m}/\text{mm}^{-1}$, 95% CI, 0.001-0.009, $P = 0.007$) (Fig 7), and GSI change ($\beta = 0.002 \mu\text{m}/\text{e}^{-3}$, 95% CI, 0.0002-0.004, $P = 0.048$) (adjustment for age, gender, and IOP). The association of the RNFL thinning with the LC shallowing was stronger in the early-to-moderate glaucoma group ($\beta = 0.031 \mu\text{m}/\mu\text{m}$, 95% CI 0.02-0.04, $P < 0.001$) than in the advanced glaucoma group ($\beta = 0.011 \mu\text{m}/\mu\text{m}$, 95% CI, 0.004-0.02, $P = 0.003$) ($P = 0.014$).

The relationships between the postoperative changes of VF parameters and the changes of LC morphologic parameters were significant only in the subgroups. After trabeculectomy the worsening of the VF pattern standard deviation (PSD) was related to the LC shallowing in the early-to-moderate glaucoma group ($\beta = 0.004 \mu\text{m}/\text{dB}$, 95% CI, 0.0004 - 0.007, $P = 0.028$), while the worsening of the VF MD showed a mild association with the positive

change of the GSI ($\beta = 0.003 \text{ dB/e}^{-3}$, 95% CI 0.0002-0.005, $P = 0.035$).

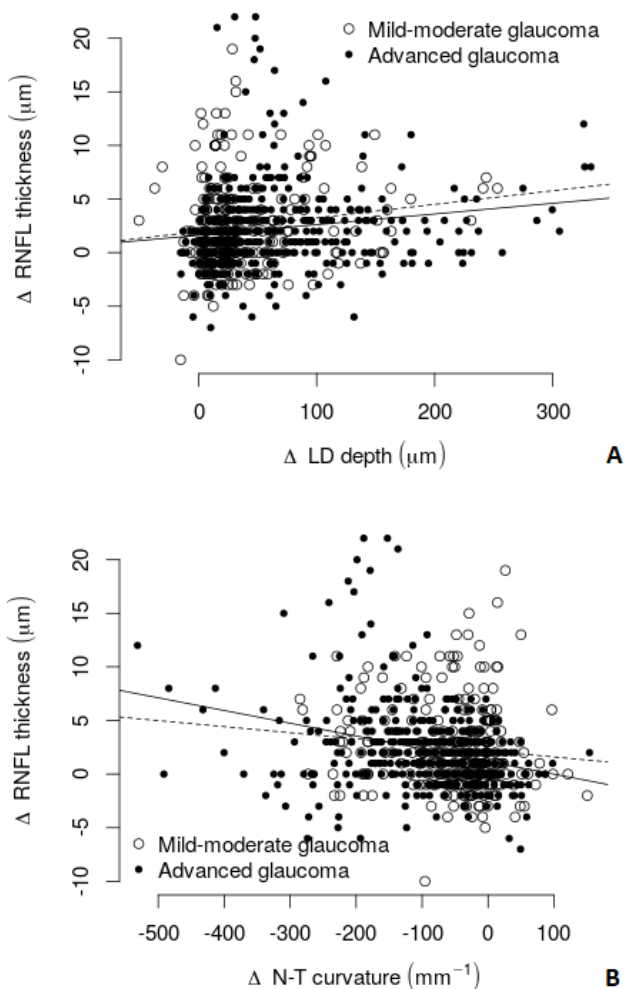


Fig. 7. A scatter plot showing the relationship between the thinning of the retinal nerve fiber layer (RNFL) with (A) a decrease in lamina cribrosa (LC) depth and (B) a flattening of nasal-temporal (N-T) curvature during a year after trabeculectomy.

Table 8. A regression analysis of factors associated with the postoperative changes of the lamina cribrosa global shape index.

Variable	Change of LC global shape index		
	Univariate β (95% CI)	P	Multivariate β (95% CI)
Age, 10 year	-0.0007 (-0.02 to 0.02)	0.952	-0.008 (-0.03 to 0.01)
Male sex	0.020 (-0.019 to 0.058)	0.324	0.028 (-0.006 to 0.062)
AL preoperative, mm	0.015 (-0.007 to 0.037)	0.175	
IOP preoperative, mmHg	-0.002 (-0.005 to 0.001)	0.186	
IOP reduction, * mmHg	-0.002 (-0.005 to 0.0001)	0.061	-0.003 (-0.006 to -0.001)
CCT preoperative, μm	0.0001 (-0.0005 to 0.0007)	0.643	
VF MD preoperative, dB	0.001 (-0.001 to 0.003)	0.306	
VF MD decrease, * dB	0.003 (-0.007 to 0.012)	0.609	
RNFL thickness preoperative, μm	0.0007 (-0.0008 to 0.002)	0.368	-0.0006 (-0.002 to 0.001)
RNFL thinning, * μm	0.005 (0.0001 to 0.009)	0.047	0.007 (0.003 to 0.012)
BMO area preoperative, μm^2	0.026 (-0.023 to 0.076)	0.302	
LCD preoperative, 100 μm	-0.02 (-0.03 to -0.004)	0.013	0.003 (-0.02 to 0.02)
N-T curvature preoperative, 100 mm^{-1}	0.006 (-0.004 to 0.02)	0.249	
S-I curvature preoperative, 100 mm^{-1}	0.007 (0.004 to 0.01)	<0.001	0.006 (0.003 to 0.01)

AL = axial length; BMO = Bruch's membrane opening; CCT = central corneal thickness; CI = confidence interval; IOP = intraocular pressure; LC = lamina cribrosa; LCD = lamina cribrosa depth; MD = mean deviation; N-T = nasal-temporal; RNFL = retinal nerve fiber layer; S-I = superior-inferior; VF = visual field. * Change at the 12th month of follow-up. In addition to age, sex, and baseline RNFL thickness, variables with $P < 0.1$ from the univariate model were included in the multivariate model. * Change at the 12th month of follow-up.

Comparison of Lamina Cribrosa Changes with respect to the Severity and Type of Glaucoma

There were no statistical differences in the age, gender, visual acuity, refractive error, baseline IOP, and IOP reduction between the groups with respect to the glaucoma diagnosis and the severity of the disease ($P > 0.05$). In the group of advanced-stage glaucoma, the central cornea thickness ($515 \pm 34 \mu\text{m}$) was less, the VF MD ($19.72 \pm 6.38 \text{ dB}$) was worse and the RNFL ($47.03 \pm 9.17 \mu\text{m}$) was thinner when compared to the group of early-to-moderate glaucoma ($529 \pm 28 \mu\text{m}$, $5.49 \pm 4.86 \text{ dB}$ and $66.63 \pm 12.67 \mu\text{m}$, respectively) ($P < 0.001$). The ocular axial length was shorter in the group of PACG ($22.73 \pm 0.52 \text{ mm}$) than in the group of POAG (23.56 ± 0.92) and PEXG (23.73 ± 0.91) ($P = 0.012$).

No differences in the LCD and GSI were found between the groups of early-to-moderate and advanced glaucoma before the trabeculectomy ($P > 0.05$). Meanwhile, the N-S curvature at baseline was greater in the eyes with the advanced disease ($-650 \pm 201 \text{ mm}^{-1}$) compared to those with early-to-moderate disease ($-554 \pm 154 \text{ mm}^{-1}$) ($P = 0.015$).

After the trabeculectomy there was a greater LC shallowing (3-10d, 1, 6, and 9 months postoperatively, $P \leq 0.045$) and N-T flattening (6, 9 and 12 months postoperatively, $P \leq 0.043$) in the advanced glaucoma group compared to the early-to-moderate glaucoma group ($68.2 \pm 66.7 \mu\text{m}$ vs $48.4 \pm 52.4 \mu\text{m}$, $P = 0.027$; $-99.9 \pm 96.4 \text{ mm}^{-1}$ v s $-60.8 \pm 80.7 \text{ mm}^{-1}$, $P = 0.043$; the change of LCD and N-T curvature after 6 months, respectively). The postoperative morphologic LC parameters did not differ significantly between the groups ($P > 0.05$).

There were no differences in the baseline LC parameters or in the postoperative changes of the LCD, curvature, and GSI between the groups of POAG, PACG, and PEXG ($P > 0.05$).

DISCUSSION

In the present study, we evaluated the quantitative shape, curvature, and positional changes of the LC in glaucoma-affected eyes during the first year after trabeculectomy. A long-term flattening of the LC curvature, as well as shallowing of mean and sectoral LCD, were observed. However, the overall LC shape, characterized by GSI, changed significantly only in the early postoperative period. To the best of our knowledge, this is the first study to describe the IOP reduction-induced changes of the actual lamina curvature and its global shape.

Thus far, the clinically measurable quantitative LC parameters related to the ONH biomechanics have been limited. Most of the studies addressing the LC morphology evaluated the position rather than the shape of the lamina. The LC was reported to be deeper in glaucomatous eyes compared with healthy ones^{24,25,70-72} and deeper LC were related to greater glaucomatous damage.²⁴⁻²⁶ However, the predominant measurement of the LC morphology was LCD, which was defined with reference to the BMO plane and therefore carried potential bias. The reason is that the BMO position is influenced by the choroidal thickness, which has been shown to vary with age, diurnal phase, and systemic health as well as after IOP reduction.^{57,58,60,73} Moreover, although the change in the LCD after the IOP reduction reflected the positional reversal of the lamina, it did not necessarily described the change in the LC curvature or shape, because the migration of the LC insertion might be possible due to active ONH remodeling.^{22,74} Examining other LC parameters characterizing its morphology independently from shifting anatomic landmarks remained an important scientific goal.

Recently, increased attention has been given to the curvature of the LC, because it describes the LC topography and is not affected by the choroidal thickness. Kim and colleagues have reported that the LC posterior bowing, expressed as a LC curvature index, was increased in primary open-angle glaucoma when compared with

healthy control subjects and in hypertension glaucoma when compared with normal tension glaucoma.^{75,76} Later, the LC curvature index was shown to have a better discriminating capability between POAG and healthy eyes than the LCD.⁷⁷ One study has addressed the effect of IOP reduction on the LC curvature.⁶¹ Lee et al. evaluated eyes with POAG after trabeculectomy and found a decrease of the LC curvature index in the horizontal ONH sections after surgical IOP reduction.⁶¹ The latter findings are in agreement with our study demonstrating the flattening of both principal LC curvatures after trabeculectomy; however, the results cannot be compared directly because in the previous study, the LC curvature index was defined as an inflection of the curve (μm) representing a section of the LC and did not correspond exactly to the actual LC curvature.⁶¹ Furthermore, the measurements were limited to seven horizontal ONH cross-sections. In our study, a circular arc was fitted to each of the LC curves of radial cross-sections at principal meridians and allowed an estimation of the LC curvature (mm^{-1}) along radial orientations in a global sense.⁶²

The LC GSI was introduced several years ago as a new morphologic parameter for characterizing the geometrical shape of the anterior lamina. LC GSI does not depend on the BMO reference plane and gives a quantitative, easily comparable value. In a healthy Indian population, the majority of the LC were reported to have the shape of a rut or saddle-rut and deeper LC insertions in the superior and inferior LC regions.⁶² The GSI was shown to be smaller (more negative) in POAG eyes than in healthy or ocular hypertensive subjects.⁶⁸ In agreement, we also found the LC to be more curved in the nasal-temporal meridian compared with the superior-inferior one and to be deeper in the superior and inferior LC sectors of glaucomatous eyes. However, our mean GSI values were smaller than previously described, indicating a shape shift toward the form of a cup. These differences are most likely attributable to a higher, long-standing IOP and more advanced glaucoma of our subjects, since the risk factors of glaucoma, such as the vertical cup-to-disc

ratio and minimum rim width, have been shown to be associated with more negative LC GSI.⁶²

In our study, the increase in LC GSI after trabeculectomy was observed only in the early postoperative period at the time of the greatest IOP reduction. It is likely that the later postoperative changes of LC curvatures in both axis occurred concomitantly, since the GSI did not change significantly. Thus, our results suggests that parameters such as LC curvature and LCD are clinically more relevant than GSI in describing the longitudinal morphologic LC changes after trabeculectomy. However, it should be noted that the GSI parameter, but not the one of LCD, has been earlier reported to change during an IOP elevation in healthy and glaucomatous eyes.⁶⁸ Furthermore, eyes with POAG tended to have a more negative GSI following acute IOP increase compared to normal subject.⁶⁸

The positional responses of the LC to IOP changes have been evaluated in experimental^{11,35,78-80} and clinical^{49-55,81-84} studies reporting anterior-posterior displacements. Many of them have observed a decrease in the mean LCD after IOP reduction.^{50-53,55,84} However, several studies have previously reported that both posterior and anterior movements of the LC can occur after IOP lowering, which is in agreement with our data.^{49,54,81-83} The different methodologies of LCD measurements and variable IOP reduction prevent any direct comparison of the magnitude of LC change between the studies. Many research groups evaluated the LCD only in a selected number of the ONH scans at the deepest, central, or paracentral locations of LC surface and reported bigger LCD values than ours.^{51,52,83-85} In our study, an improved LC visibility after adaptive compensation and custom-written software allowed us to cover approximately 90% of the lamina surface and to assess the mean LCD including peripheral LC. The high coverage of LC also enabled us to measure the sectoral LCD. We found the LCD to decrease more in the superior and inferior sectors when compared with the temporal segment. The smaller density of the supporting connective tissue and glial cells in the superior and inferior quadrants

have been reported and could explain the sectoral differences in LC mobility.⁸⁶

The mean postsurgical LCD in our study is similar to the baseline data of Tun et al., who evaluated LCD after IOP elevation in glaucomatous eyes using the same methodology.⁶⁸ The LCD change that we found is also comparable to the results of the study reporting the LC shallowing after trabeculectomy or deep sclerectomy in POAG eyes with at least $\frac{3}{4}$ of ONH area measured.⁵⁰ We observed the mean LCD to decrease until the sixth postoperative month, and, thereafter, the LC position stabilized. These results are consistent with other authors reporting a similar tendency over a 2-year follow-up period.^{52,82} Because IOP did not differ significantly between the visits after the first postoperative month, the subsequent changes of LCD and LC curvatures are likely to be a result of connective tissue remodeling and collagen arrangement under new postoperative hydrostatic pressure circumstances.^{22,87}

We have observed the inward and outward movements of the LC after trabeculectomy. In the majority of our patients, the LC became shallower. However, there was a small group of the eyes that displayed a deepening of the LC. Most of the cases with deeper LC compared with the baseline occurred within the first postoperative month and reduced in number over time. Such a bidirectional biomechanical response of the LC to IOP change is a consequence of 2 major forces: the translaminar pressure gradient and IOP induced circumferential forces of the peripapillary sclera affecting the LC.¹⁷ Because of the decrease in translaminar and transscleral pressure gradients, we would assume the shallowing of the LC and inward movement of the peripapillary sclera after the IOP reduction. However, because the surrounding sclera and LC respond as a single unit, the altered scleral forces can subsequently influence the stresses and strains on the LC and, thus, induce its outward movement. The biomechanical behavior of LC and peripapillary sclera is not fully understood because of the complex interaction between the IOP, material properties, and the geometry of LC and sclera.³⁴ This

biomechanical variability of the LC is in agreement with model predictions by Sigal et al., where the increase in LCD after IOP lowering could be explained by a reduction in scleral canal size, leading to the posterior movement of the LC.⁸⁸ Previous clinical studies have corroborated our findings that the LC moves anteriorly or posteriorly after a decrease in IOP.^{54,82,83,89} Quigley et al. showed that the anterior LC position became shallower or deeper or stayed unchanged with IOP reduction.⁵⁴ The displacement of LCD was greater at lower IOP but was not associated with the magnitude of IOP lowering. Girard et al. evaluated the 3-dimensional ONH displacements and strain relief in vivo and found that the LC displaced posteriorly, anteriorly, or not at all; however, no factors related to different LC behavior were identified.⁸⁹ In our study, we demonstrated that eyes with shallower LCD compared with baseline responded to IOP reduction with greater movement anteriorly than eyes with deeper LCD.

We also evaluated the relationships of the morphologic LC changes and their possible predictors. A younger age was a significant factor for the greater flattening and shallowing of the postoperative LC. The age-related differences in the extracellular matrix of the sclera and LC potentially leading to the changes in their material properties have been reported and could at least partly explain this association.⁹⁰ Studies in animal and human eyes have demonstrated that the sclera becomes stiffer with age and therefore is subject to higher stresses but lower strains at different levels of IOP.⁹¹⁻⁹⁴ Albon et al. showed age-related changes in the collagenous and non-collagenous components of the LC and observed that the mechanical compliance of the human LC decreased with age.^{95,96} However, because the biomechanics of the LC and sclera are highly interdependent, it is difficult to isolate the effects on the biomechanical properties of the LC alone. The reduction of IOP was also associated with a decrease in LCD, curvature, and GSI after the surgery. Our findings are in agreement with the studies reporting younger age and larger IOP reduction to be related to greater changes

in the LCD and LC curve after trabeculectomy^{51,53,61,83,84,97,98} However, it should be mentioned that in some studies, the IOP association was not confirmed, potentially because of a smaller sample size and less IOP reduction.^{54,55,97} Quigley et al. showed that the LCD change was more related to the level of IOP than to the magnitude of IOP change.⁵⁴

We found RNFL thinning to be associated with greater changes in the LCD, curvature, and shape during one year after trabeculectomy. Similar results concerning the postoperative LCD changes and RNFL thinning in POAG patients have been recently reported.^{50,81} Regardless of the performed procedure (a trabeculectomy or a non-penetrating deep sclerectomy), the magnitude of the decrease in the LCD was associated with significant focal RNFL thinning.⁵⁰ Furthermore, after the postoperative follow-up of 12 to 29 months, the authors concluded that a thinner RNFL thickness after glaucoma surgery was associated with a greater rate of the LCD reduction, not with position of the LC at the final visit.⁸¹ Lee et al., however, found no relationship between the postoperative changes of the LCD and rate of RNFL thinning. The authors concluded that eyes with sustained LCD reduction over a long period had a slow rate of progressive RNFL thinning after trabeculectomy.⁸²

Intuitively, the shallowing (anterior movement) of the LC after trabeculectomy is related to a relief of compressed axons of the optic nerve when compared to the preoperative condition. Strains of the ONH have been in vivo shown to be relieved after trabeculectomy.⁸⁹ However, the data about the positive association between the postoperative RNFL thinning with the magnitude and rate of LCD change suggest that a rapid and significant anterior LC re-displacement after glaucoma surgery can itself be potentially related to the damage of axons, which pass through the distorted LC pores. To the best of our knowledge, no other study has reported the association between the changes in the LC curvature and global shape with the glaucoma progression after the surgical IOP reduction.

In our study, the morphologic LC changes after trabeculectomy were greater in the group of advanced glaucoma compared to the group of early-to-moderate disease. Since the demographic parameters and reduction of IOP did not differ significantly between the groups, we hypothesize that several factors, including progression-associated LC thinning^{85,99,100} and the potential changes in the material properties of LC in advanced-stage disease, might play a role in the different biomechanical response.

The semi-automated measurements of the global LC shape and the actual geometrical curvature, as well as the prospective design of the study with a long follow-up period, are the obvious strengths of our study. However, we should note some potential limitations. First, we performed only a horizontal scanning of the ONH, and the superior and inferior lamina were poorly visualized in a part of the peripheral scans. The mean LC visibility of the 130 enrolled eyes was 89.8%, which may be improved if one uses a radial scan approach. To minimize the limitation, only scans with LC visibility better than 70% (mean 92.4%) were analyzed. Second, the LC curvatures were measured only in two meridians, whereas the superior-temporal and inferior-temporal regions, which are prone to glaucomatous injury, were not evaluated. However, it has been previously reported that the sections containing the principal arc curvatures of LC are aligned to the vertical and horizontal directions.⁶² Furthermore, a comparison of the GSI values, computed from the entire reconstructed LC with the GSI values based on the N-T and S-I curvatures, showed very good agreement.⁶² These results suggest that an evaluation of the vertical and horizontal meridians alone would be sufficient to calculate the GSI representing the LC global anterior shape. Third, the GSI was evaluated globally by fitting the arc curvature to the entire cross-section; thus, it did not reflect the local changes of LC shape. However, no widely accepted globally and locally sensitive parameter for LC geometry is available. Fourth, the mean and sectoral postoperative LCD measurements could be affected by the changing choroidal thickness,

as was described previously.⁶⁰ Fifth, since the majority of the glaucoma surgery patients had the pseudoexfoliative syndrome, the study sample mostly reflected the morphologic changes of LC in the pseudoexfoliative glaucoma. This could have potentially influenced the results of the LC biomechanical response if considering a possible pseudoexfoliation-specific elastinopathy of the LC and the findings that the lamina is thinner and less stiff in eyes with the pseudoexfoliation syndrome.^{101,102} Further studies are needed to overcome these limitations and to investigate the long-term structural changes of the post-trabeculectomy LC morphology and its association with glaucomatous injury.

CONCLUSIONS

1. In most eyes, trabeculectomy resulted in a long-term flattening and shallowing of the lamina cribrosa, which tended to stabilize after 6 months. Notably, in some eyes, the lamina cribrosa deepened from baseline, revealing bidirectional behavior after the surgery. Changes in the global shape of the lamina cribrosa appeared to be temporal.
2. Reduction of intraocular pressure played an important role in the early phase of postoperative lamina cribrosa change. However, in the later phase, the remodeling of the lamina cribrosa may have played a crucial role, with intraocular pressure being stable.
3. The greater morphologic changes of the lamina cribrosa after trabeculectomy were significantly related to the structural and functional progression of glaucoma, with the relationship being influenced by the severity of the disease.
4. The biomechanical response of the lamina cribrosa to trabeculectomy was associated with other intraocular-pressure-dependent structural changes – an axial length shortening as well as choroidal and macular thickening. The changes of the depth, curvature, and global shape of the lamina cribrosa positively correlated in-between and with the magnitude of the corresponding morphologic parameter at baseline. A younger age had a positive effect on the flattening and shallowing of the lamina cribrosa.
5. Eyes with advanced glaucoma tended to have a more curved lamina cribrosa at baseline and showed a greater reversal of the lamina cribrosa curvature and depth following trabeculectomy compared to the earlier stages of glaucoma.

PRACTICAL RECOMMENDATIONS

1. An enhanced depth imaging spectral domain optical coherence tomography enables visualization of the deep ocular structures, including the lamina cribrosa and choroid. This imaging benefits to objective analysis and documentation of the morphologic characteristics of the mentioned ocular structures.
2. Morphology 1.0 software is useful for a quantitative evaluation of the anterior surface of the lamina cribrosa. A complex morphologic assessment of the lamina is valuable for glaucoma research since it provides comprehensive knowledge about the geometry and biomechanics of the lamina cribrosa, which is relevant to insights into the mechanisms of glaucoma pathogenesis.
3. Trabeculectomy should aim for a safe target intraocular pressure of the patient, avoiding inappropriately low postoperative levels. Inadequately high surgical reduction of intraocular pressure could lead to a considerable and abrupt shallowing and flattening of the lamina cribrosa, which, in the long-term, is related to the progression of glaucoma.

REFERENCES

1. Jonas JB, Aung T, Bourne RR, Bron AM, Ritch R, Panda-Jonas S. Glaucoma. *Lancet (London, England)*. 2017;390(10108):2183-2193.
2. Flaxman SR, Bourne RRA, Resnikoff S, et al. Global causes of blindness and distance vision impairment 1990-2020: a systematic review and meta-analysis. *The Lancet Global health*. 2017;5(12):e1221-e1234.
3. Lee PP, Kelly SP, Mills RP, et al. Glaucoma in the United States and Europe: predicting costs and surgical rates based upon stage of disease. *Journal of glaucoma*. 2007;16(5):471-478.
4. Tham YC, Li X, Wong TY, Quigley HA, Aung T, Cheng CY. Global prevalence of glaucoma and projections of glaucoma burden through 2040: a systematic review and meta-analysis. *Ophthalmology*. 2014;121(11):2081-2090.
5. Quigley HA, Broman AT. The number of people with glaucoma worldwide in 2010 and 2020. *The British journal of ophthalmology*. 2006;90(3):262-267.
6. Comparison of glaucomatous progression between untreated patients with normal-tension glaucoma and patients with therapeutically reduced intraocular pressures. Collaborative Normal-Tension Glaucoma Study Group. *American journal of ophthalmology*. 1998;126(4):487-497.
7. The Advanced Glaucoma Intervention Study (AGIS): 7. The relationship between control of intraocular pressure and visual field deterioration. The AGIS Investigators. *American journal of ophthalmology*. 2000;130(4):429-440.
8. Heijl A, Leske MC, Bengtsson B, Hyman L, Bengtsson B, Hussein M. Reduction of intraocular pressure and glaucoma progression: results from the Early Manifest Glaucoma Trial. *Archives of ophthalmology (Chicago, Ill : 1960)*. 2002;120(10):1268-1279.
9. Kass MA, Heuer DK, Higginbotham EJ, et al. The Ocular Hypertension Treatment Study: a randomized trial determines that topical ocular hypotensive medication delays or prevents the onset of primary open-angle glaucoma.

- Archives of ophthalmology (Chicago, Ill : 1960)*. 2002;120(6):701-713; discussion 829-730.
10. Musch DC, Gillespie BW, Niziol LM, Lichter PR, Varma R. Intraocular pressure control and long-term visual field loss in the Collaborative Initial Glaucoma Treatment Study. *Ophthalmology*. 2011;118(9):1766-1773.
 11. Bellezza AJ, Rintalan CJ, Thompson HW, Downs JC, Hart RT, Burgoyne CF. Deformation of the lamina cribrosa and anterior scleral canal wall in early experimental glaucoma. *Investigative ophthalmology & visual science*. 2003;44(2):623-637.
 12. Burgoyne CF, Downs JC, Bellezza AJ, Hart RT. Three-dimensional reconstruction of normal and early glaucoma monkey optic nerve head connective tissues. *Investigative ophthalmology & visual science*. 2004;45(12):4388-4399.
 13. Quigley HA, Addicks EM, Green WR, Maumenee AE. Optic nerve damage in human glaucoma. II. The site of injury and susceptibility to damage. *Archives of ophthalmology (Chicago, Ill : 1960)*. 1981;99(4):635-649.
 14. Howell GR, Libby RT, Jakobs TC, et al. Axons of retinal ganglion cells are insulated in the optic nerve early in DBA/2J glaucoma. *The Journal of cell biology*. 2007;179(7):1523-1537.
 15. Lockwood H, Reynaud J, Gardiner S, et al. Lamina cribrosa microarchitecture in normal monkey eyes part 1: methods and initial results. *Investigative ophthalmology & visual science*. 2015;56(3):1618-1637.
 16. Yang H, Ren R, Lockwood H, et al. The Connective Tissue Components of Optic Nerve Head Cupping in Monkey Experimental Glaucoma Part 1: Global Change. *Investigative ophthalmology & visual science*. 2015;56(13):7661-7678.
 17. Burgoyne CF. A biomechanical paradigm for axonal insult within the optic nerve head in aging and glaucoma. *Experimental eye research*. 2011;93(2):120-132.
 18. Campbell IC, Coudrillier B, Ross Ethier C. Biomechanics of the posterior eye: a critical role in health and disease. *Journal of biomechanical engineering*. 2014;136(2):021005.

19. Sigal IA, Flanagan JG, Ethier CR. Factors influencing optic nerve head biomechanics. *Investigative ophthalmology & visual science*. 2005;46(11):4189-4199.
20. Sigal IA, Ethier CR. Biomechanics of the optic nerve head. *Experimental eye research*. 2009;88(4):799-807.
21. Burgoyne CF, Downs JC, Bellezza AJ, Suh JK, Hart RT. The optic nerve head as a biomechanical structure: a new paradigm for understanding the role of IOP-related stress and strain in the pathophysiology of glaucomatous optic nerve head damage. *Progress in retinal and eye research*. 2005;24(1):39-73.
22. Crawford Downs J, Roberts MD, Sigal IA. Glaucomatous cupping of the lamina cribrosa: a review of the evidence for active progressive remodeling as a mechanism. *Experimental eye research*. 2011;93(2):133-140.
23. Downs JC, Roberts MD, Burgoyne CF. Mechanical environment of the optic nerve head in glaucoma. *Optometry and vision science : official publication of the American Academy of Optometry*. 2008;85(6):425-435.
24. Furlanetto RL, Park SC, Damle UJ, et al. Posterior displacement of the lamina cribrosa in glaucoma: in vivo interindividual and intereye comparisons. *Investigative ophthalmology & visual science*. 2013;54(7):4836-4842.
25. Jung KI, Jung Y, Park KT, Park CK. Factors affecting plastic lamina cribrosa displacement in glaucoma patients. *Investigative ophthalmology & visual science*. 2014;55(12):7709-7715.
26. Ren R, Yang H, Gardiner SK, et al. Anterior lamina cribrosa surface depth, age, and visual field sensitivity in the Portland Progression Project. *Investigative ophthalmology & visual science*. 2014;55(3):1531-1539.
27. Albon J, Farrant S, Akhtar S, et al. Connective tissue structure of the tree shrew optic nerve and associated ageing changes. *Investigative ophthalmology & visual science*. 2007;48(5):2134-2144.
28. Fatehee N, Yu PK, Morgan WH, Cringle SJ, Yu DY. The impact of acutely elevated intraocular pressure on the porcine optic nerve head. *Investigative ophthalmology & visual science*. 2011;52(9):6192-6198.

29. Jonas JB, Mardin CY, Schlotzer-Schrehardt U, Naumann GO. Morphometry of the human lamina cribrosa surface. *Investigative ophthalmology & visual science*. 1991;32(2):401-405.
30. Levy NS, Crapps EE. Displacement of optic nerve head in response to short-term intraocular pressure elevation in human eyes. *Archives of ophthalmology (Chicago, Ill : 1960)*. 1984;102(5):782-786.
31. Sigal IA, Flanagan JG, Tertinegg I, Ethier CR. Finite element modeling of optic nerve head biomechanics. *Investigative ophthalmology & visual science*. 2004;45(12):4378-4387.
32. Sigal IA, Flanagan JG, Tertinegg I, Ethier CR. Modeling individual-specific human optic nerve head biomechanics. Part I: IOP-induced deformations and influence of geometry. *Biomechanics and modeling in mechanobiology*. 2009;8(2):85-98.
33. Sigal IA, Flanagan JG, Tertinegg I, Ethier CR. Modeling individual-specific human optic nerve head biomechanics. Part II: influence of material properties. *Biomechanics and modeling in mechanobiology*. 2009;8(2):99-109.
34. Sigal IA, Yang H, Roberts MD, Burgoyne CF, Downs JC. IOP-induced lamina cribrosa displacement and scleral canal expansion: an analysis of factor interactions using parameterized eye-specific models. *Investigative ophthalmology & visual science*. 2011;52(3):1896-1907.
35. Yan DB, Coloma FM, Metheetrairut A, Trope GE, Heathcote JG, Ethier CR. Deformation of the lamina cribrosa by elevated intraocular pressure. *The British journal of ophthalmology*. 1994;78(8):643-648.
36. Spaide RF, Koizumi H, Pozzoni MC. Enhanced depth imaging spectral-domain optical coherence tomography. *American journal of ophthalmology*. 2008;146(4):496-500.
37. Wang B, Nevins JE, Nadler Z, et al. In vivo lamina cribrosa micro-architecture in healthy and glaucomatous eyes as assessed by optical coherence tomography. *Investigative ophthalmology & visual science*. 2013;54(13):8270-8274.
38. Nadler Z, Wang B, Wollstein G, et al. Repeatability of in vivo 3D lamina cribrosa microarchitecture using adaptive

- optics spectral domain optical coherence tomography. *Biomedical optics express*. 2014;5(4):1114-1123.
39. Lee EJ, Kim TW, Weinreb RN, Park KH, Kim SH, Kim DM. Visualization of the lamina cribrosa using enhanced depth imaging spectral-domain optical coherence tomography. *American journal of ophthalmology*. 2011;152(1):87-95.e81.
40. Choma M, Sarunic M, Yang C, Izatt J. Sensitivity advantage of swept source and Fourier domain optical coherence tomography. *Optics express*. 2003;11(18):2183-2189.
41. Sigal IA, Wang B, Strouthidis NG, Akagi T, Girard MJ. Recent advances in OCT imaging of the lamina cribrosa. *The British journal of ophthalmology*. 2014;98 Suppl 2:ii34-39.
42. Park HY, Jeon SH, Park CK. Enhanced depth imaging detects lamina cribrosa thickness differences in normal tension glaucoma and primary open-angle glaucoma. *Ophthalmology*. 2012;119(1):10-20.
43. Park HY, Park CK. Diagnostic capability of lamina cribrosa thickness by enhanced depth imaging and factors affecting thickness in patients with glaucoma. *Ophthalmology*. 2013;120(4):745-752.
44. Park SC, Hsu AT, Su D, et al. Factors associated with focal lamina cribrosa defects in glaucoma. *Investigative ophthalmology & visual science*. 2013;54(13):8401-8407.
45. You JY, Park SC, Su D, Teng CC, Liebmann JM, Ritch R. Focal lamina cribrosa defects associated with glaucomatous rim thinning and acquired pits. *JAMA ophthalmology*. 2013;131(3):314-320.
46. Faridi OS, Park SC, Kabadi R, et al. Effect of focal lamina cribrosa defect on glaucomatous visual field progression. *Ophthalmology*. 2014;121(8):1524-1530.
47. Kiumehr S, Park SC, Cyril D, et al. In vivo evaluation of focal lamina cribrosa defects in glaucoma. *Archives of ophthalmology (Chicago, Ill : 1960)*. 2012;130(5):552-559.
48. Agoumi Y, Sharpe GP, Hutchison DM, Nicoleta MT, Artes PH, Chauhan BC. Laminar and prelaminar tissue displacement during intraocular pressure elevation in glaucoma patients and healthy controls. *Ophthalmology*. 2011;118(1):52-59.

49. Esfandiari H, Efatizadeh A, Hassanpour K, Doozandeh A, Yaseri M, Loewen NA. Factors associated with lamina cribrosa displacement after trabeculectomy measured by optical coherence tomography in advanced primary open-angle glaucoma. *Graefes Arch Clin Exp Ophthalmol.* 2018;256(12):2391-2398.
50. Krzyzanowska-Berkowska P, Melinska A, Helemejko I, Robert Iskander D. Evaluating displacement of lamina cribrosa following glaucoma surgery. *Graefes Arch Clin Exp Ophthalmol.* 2018;256(4):791-800.
51. Lee EJ, Kim TW, Weinreb RN. Reversal of lamina cribrosa displacement and thickness after trabeculectomy in glaucoma. *Ophthalmology.* 2012;119(7):1359-1366.
52. Lee EJ, Kim TW, Weinreb RN. Variation of lamina cribrosa depth following trabeculectomy. *Investigative ophthalmology & visual science.* 2013;54(8):5392-5399.
53. Park HY, Shin HY, Jung KI, Park CK. Changes in the lamina and prelamina after intraocular pressure reduction in patients with primary open-angle glaucoma and acute primary angle-closure. *Investigative ophthalmology & visual science.* 2014;55(1):233-239.
54. Quigley H, Arora K, Idrees S, et al. Biomechanical Responses of Lamina Cribrosa to Intraocular Pressure Change Assessed by Optical Coherence Tomography in Glaucoma Eyes. *Investigative ophthalmology & visual science.* 2017;58(5):2566-2577.
55. Reis AS, O'Leary N, Stanfield MJ, Shuba LM, Nicolela MT, Chauhan BC. Laminar displacement and prelamina tissue thickness change after glaucoma surgery imaged with optical coherence tomography. *Investigative ophthalmology & visual science.* 2012;53(9):5819-5826.
56. Yoshikawa M, Akagi T, Nakanishi H, et al. Longitudinal change in choroidal thickness after trabeculectomy in primary open-angle glaucoma patients. *Japanese journal of ophthalmology.* 2017;61(1):105-112.
57. Chakraborty R, Read SA, Collins MJ. Diurnal variations in axial length, choroidal thickness, intraocular pressure, and ocular biometrics. *Investigative ophthalmology & visual science.* 2011;52(8):5121-5129.

58. Johnstone J, Fazio M, Rojananuangnit K, et al. Variation of the axial location of Bruch's membrane opening with age, choroidal thickness, and race. *Investigative ophthalmology & visual science*. 2014;55(3):2004-2009.
59. Lee SW, Yu SY, Seo KH, Kim ES, Kwak HW. Diurnal variation in choroidal thickness in relation to sex, axial length, and baseline choroidal thickness in healthy Korean subjects. *Retina (Philadelphia, Pa)*. 2014;34(2):385-393.
60. Tan KA, Gupta P, Agarwal A, et al. State of science: Choroidal thickness and systemic health. *Survey of ophthalmology*. 2016;61(5):566-581.
61. Lee SH, Yu DA, Kim TW, Lee EJ, Girard MJ, Mari JM. Reduction of the Lamina Cribrosa Curvature After Trabeculectomy in Glaucoma. *Investigative ophthalmology & visual science*. 2016;57(11):5006-5014.
62. Thakku SG, Tham YC, Baskaran M, et al. A Global Shape Index to Characterize Anterior Lamina Cribrosa Morphology and Its Determinants in Healthy Indian Eyes. *Investigative ophthalmology & visual science*. 2015;56(6):3604-3614.
63. Hitchings R. *Terminology and Guidelines for Glaucoma*. 4th edition. Italy: European Glaucoma Society; 2014.
64. Susanna R, Jr., Vessani RM. Staging glaucoma patient: why and how? *The open ophthalmology journal*. 2009;3:59-64.
65. Girard MJ, Strouthidis NG, Ethier CR, Mari JM. Shadow removal and contrast enhancement in optical coherence tomography images of the human optic nerve head. *Investigative ophthalmology & visual science*. 2011;52(10):7738-7748.
66. Girard MJ, Tun TA, Husain R, et al. Lamina cribrosa visibility using optical coherence tomography: comparison of devices and effects of image enhancement techniques. *Investigative ophthalmology & visual science*. 2015;56(2):865-874.
67. Mari JM, Strouthidis NG, Park SC, Girard MJ. Enhancement of lamina cribrosa visibility in optical coherence tomography images using adaptive compensation. *Investigative ophthalmology & visual science*. 2013;54(3):2238-2247.
68. Tun TA, Thakku SG, Png O, et al. Shape Changes of the Anterior Lamina Cribrosa in Normal, Ocular Hypertensive,

- and Glaucomatous Eyes Following Acute Intraocular Pressure Elevation. *Investigative ophthalmology & visual science*. 2016;57(11):4869-4877.
69. Faul F, Erdfelder E, Lang AG, Buchner A. G*Power 3: a flexible statistical power analysis program for the social, behavioral, and biomedical sciences. *Behavior research methods*. 2007;39(2):175-191.
70. Kim YW, Kim DW, Jeoung JW, Kim DM, Park KH. Peripheral lamina cribrosa depth in primary open-angle glaucoma: a swept-source optical coherence tomography study of lamina cribrosa. *Eye (London, England)*. 2015;29(10):1368-1374.
71. Park SC, Brumm J, Furlanetto RL, et al. Lamina cribrosa depth in different stages of glaucoma. *Investigative ophthalmology & visual science*. 2015;56(3):2059-2064.
72. Li L, Bian A, Cheng G, Zhou Q. Posterior displacement of the lamina cribrosa in normal-tension and high-tension glaucoma. *Acta ophthalmologica*. 2016;94(6):e492-500.
73. Kadziauskiene A, Kuoliene K, Asoklis R, Lesinskas E, Schmetterer L. Changes in choroidal thickness after intraocular pressure reduction following trabeculectomy. *Acta ophthalmologica*. 2016;94(6):586-591.
74. Yang H, Williams G, Downs JC, et al. Posterior (outward) migration of the lamina cribrosa and early cupping in monkey experimental glaucoma. *Investigative ophthalmology & visual science*. 2011;52(10):7109-7121.
75. Kim YW, Jeoung JW, Girard MJ, Mari JM, Park KH. Positional and Curvature Difference of Lamina Cribrosa According to the Baseline Intraocular Pressure in Primary Open-Angle Glaucoma: A Swept-Source Optical Coherence Tomography (SS-OCT) Study. *PloS one*. 2016;11(9):e0162182.
76. Kim YW, Jeoung JW, Kim DW, et al. Clinical Assessment of Lamina Cribrosa Curvature in Eyes with Primary Open-Angle Glaucoma. *PloS one*. 2016;11(3):e0150260.
77. Lee SH, Kim TW, Lee EJ, Girard MJ, Mari JM. Diagnostic Power of Lamina Cribrosa Depth and Curvature in Glaucoma. *Investigative ophthalmology & visual science*. 2017;58(2):755-762.

78. Strouthidis NG, Fortune B, Yang H, Sigal IA, Burgoyne CF. Longitudinal change detected by spectral domain optical coherence tomography in the optic nerve head and peripapillary retina in experimental glaucoma. *Investigative ophthalmology & visual science*. 2011;52(3):1206-1219.
79. Strouthidis NG, Fortune B, Yang H, Sigal IA, Burgoyne CF. Effect of acute intraocular pressure elevation on the monkey optic nerve head as detected by spectral domain optical coherence tomography. *Investigative ophthalmology & visual science*. 2011;52(13):9431-9437.
80. Yang H, Downs JC, Sigal IA, Roberts MD, Thompson H, Burgoyne CF. Deformation of the normal monkey optic nerve head connective tissue after acute IOP elevation within 3-D histomorphometric reconstructions. *Investigative ophthalmology & visual science*. 2009;50(12):5785-5799.
81. Krzyzanowska-Berkowska P, Czajor K, Helemejko I, Iskander DR. Relationship between the rate of change in lamina cribrosa depth and the rate of retinal nerve fiber layer thinning following glaucoma surgery. *PloS one*. 2018;13(11):e0206040.
82. Lee EJ, Kim TW. Lamina Cribrosa Reversal after Trabeculectomy and the Rate of Progressive Retinal Nerve Fiber Layer Thinning. *Ophthalmology*. 2015;122(11):2234-2242.
83. Lee EJ, Kim TW, Weinreb RN, Kim H. Reversal of lamina cribrosa displacement after intraocular pressure reduction in open-angle glaucoma. *Ophthalmology*. 2013;120(3):553-559.
84. Yoshikawa M, Akagi T, Hangai M, et al. Alterations in the neural and connective tissue components of glaucomatous cupping after glaucoma surgery using swept-source optical coherence tomography. *Investigative ophthalmology & visual science*. 2014;55(1):477-484.
85. Lee EJ, Kim TW, Kim M, Kim H. Influence of lamina cribrosa thickness and depth on the rate of progressive retinal nerve fiber layer thinning. *Ophthalmology*. 2015;122(4):721-729.

86. Radius RL. Regional specificity in anatomy at the lamina cribrosa. *Archives of ophthalmology (Chicago, Ill : 1960)*. 1981;99(3):478-480.
87. Hernandez MR. The optic nerve head in glaucoma: role of astrocytes in tissue remodeling. *Progress in retinal and eye research*. 2000;19(3):297-321.
88. Sigal IA, Yang H, Roberts MD, et al. IOP-induced lamina cribrosa deformation and scleral canal expansion: independent or related? *Investigative ophthalmology & visual science*. 2011;52(12):9023-9032.
89. Girard MJ, Beotra MR, Chin KS, et al. In Vivo 3-Dimensional Strain Mapping of the Optic Nerve Head Following Intraocular Pressure Lowering by Trabeculectomy. *Ophthalmology*. 2016;123(6):1190-1200.
90. Liu B, McNally S, Kilpatrick JI, Jarvis SP, O'Brien CJ. Aging and ocular tissue stiffness in glaucoma. *Survey of ophthalmology*. 2018;63(1):56-74.
91. Coudrillier B, Tian J, Alexander S, Myers KM, Quigley HA, Nguyen TD. Biomechanics of the human posterior sclera: age- and glaucoma-related changes measured using inflation testing. *Investigative ophthalmology & visual science*. 2012;53(4):1714-1728.
92. Geraghty B, Jones SW, Rama P, Akhtar R, Elsheikh A. Age-related variations in the biomechanical properties of human sclera. *Journal of the mechanical behavior of biomedical materials*. 2012;16:181-191.
93. Girard MJ, Suh JK, Bottlang M, Burgoyne CF, Downs JC. Scleral biomechanics in the aging monkey eye. *Investigative ophthalmology & visual science*. 2009;50(11):5226-5237.
94. Grytz R, Fazio MA, Libertiaux V, et al. Age- and race-related differences in human scleral material properties. *Investigative ophthalmology & visual science*. 2014;55(12):8163-8172.
95. Albon J, Karwatowski WS, Avery N, Easty DL, Duance VC. Changes in the collagenous matrix of the aging human lamina cribrosa. *The British journal of ophthalmology*. 1995;79(4):368-375.

96. Albon J, Purslow PP, Karwatowski WS, Easty DL. Age related compliance of the lamina cribrosa in human eyes. *The British journal of ophthalmology*. 2000;84(3):318-323.
97. Barrancos C, Rebolleda G, Oblanca N, Cabarga C, Munoz-Negrete FJ. Changes in lamina cribrosa and prelaminar tissue after deep sclerectomy. *Eye (London, England)*. 2014;28(1):58-65.
98. Diez-Alvarez L, Munoz-Negrete FJ, Casas-Llera P, Oblanca N, de Juan V, Rebolleda G. Relationship between corneal biomechanical properties and optic nerve head changes after deep sclerectomy. *European journal of ophthalmology*. 2017;27(5):535-541.
99. Chung HS, Sung KR, Lee JY, Na JH. Lamina Cribrosa-Related Parameters Assessed by Optical Coherence Tomography for Prediction of Future Glaucoma Progression. *Curr Eye Res*. 2016;41(6):806-813.
100. Omodaka K, Takahashi S, Matsumoto A, et al. Clinical Factors Associated with Lamina Cribrosa Thickness in Patients with Glaucoma, as Measured with Swept Source Optical Coherence Tomography. *PLoS one*. 2016;11(4):e0153707.
101. Kim S, Sung KR, Lee JR, Lee KS. Evaluation of lamina cribrosa in pseudoexfoliation syndrome using spectral-domain optical coherence tomography enhanced depth imaging. *Ophthalmology*. 2013;120(9):1798-1803.
102. Brauns mann C, Hammer CM, Rheinlaender J, Kruse FE, Schaffer TE, Schlotzer-Schrehardt U. Evaluation of lamina cribrosa and peripapillary sclera stiffness in pseudoexfoliation and normal eyes by atomic force microscopy. *Investigative ophthalmology & visual science*. 2012;53(6):2960-2967.

APPROBATION OF THE RESULTS

Publications

1. Kadziauskienė A, Jašinskienė E, Ašoklis R, Lesinskas E, Rekašius T, Chua J, Cheng CY, Mari JM, Girard MJA, Schmetterer L. Long-Term shape, curvature, and depth changes of the lamina cribrosa after trabeculectomy. *Ophthalmology*. 2018 Nov;125(11):1729–1740.
2. Kadziauskienė A, Kuolienė K, Ašoklis R, Lesinskas E, Schmetterer L. Changes in choroidal thickness after intraocular pressure reduction following trabeculectomy. *Acta Ophthalmologica*. 2016 Sep;94(6):586–91.
3. Kadziauskienė A, Strelkauskaitė E, Mockevičiūtė E, Ašoklis R, Lesinskas E, Schmetterer L. Changes in macular thickness after trabeculectomy with or without adjunctive 5-fluorouracil. *Acta Medica Lituanica*. 2017;24(2):93–100.

Oral Presentations and Posters

1. Kadziauskienė A., Jašinskienė E., Ašoklis R., Lesinskas E., Schmetterer L. “The Displacement of Lamina Cribrosa after Glaucoma Surgery.” Poster. International conference “Evolutionary Medicine: Health and Diseases in a Changing Environment,” June 5–8, 2018, Vilnius, Lithuania.
2. Kadziauskienė A., Strelkauskaitė E., Ašoklis R., Lesinskas E., Girard M.J.A., Schmetterer L. “The Shape and Positional Changes of Lamina Cribrosa after Trabeculectomy in Pseudoexfoliative and Primary Open Angle Glaucoma.” Poster. International conference “European Association for Vision and Eye Research Congress 2017 (EVER).” September 27–30, 2017, Nice, France.
3. Drukteinienė E., Kadziauskienė A., Strelkauskaitė E., Ašoklis R., Lesinskas E., Schmetterer L. “Macular Thickness after Intraocular

- Pressure Reduction following Trabeculectomy.” Poster. International conference “European Association for Vision and Eye Research Congress 2017 (EVER).” September 27–30, 2017, Nice, France.
4. Kadziauskienė A. “Akytoji plokštelė ir glaukoma.” Oral presentation. Conference “Metinė Lietuvos akių ligų gydytojų draugijos konferencija.” September 22–23, 2017, Kaunas, Lithuania.
 5. Kadziauskienė A., Strelkauskaitė E., Ašoklis R., Schmetterer L. “Struktūriniai akytosios plokštelės pokyčiai po trabekulektomijos.” Oral presentation. Conference “Glaukomų perspektyva: vakar, šiandien, rytoj.” May 19, 2017, Kaunas, Lithuania.
 6. Kadziauskiene A., Strelkauskaitė E., Ašoklis R., Lesinskas E., Schmetterer L. “Lamina Cribrosa Displacement following Trabeculectomy in Pseudoexfoliation and Primary Open Angle Glaucoma.” Poster. International conference “European Association for Vision and Eye Research Congress 2016 (EVER).” October 5–8, 2016, Nice, France.
 7. Kadziauskienė A., Ašoklis R., Schmetterer L. “Gyslainės storio pokyčiai po trabekulektomijos sąlygoto akispūdžio sumažėjimo.” Oral presentation. Conference “Metinė Lietuvos akių ligų gydytojų draugijos konferencija.” September 23–24, 2016, Vilnius, Lithuania.
 8. Kadziauskienė A., Kuolienė K., Galgauskas S., Ašoklis R. “Choroidal Thickness Changes after Trabeculectomy.” Poster. International conference “European Association for Vision and Eye Research Congress 2015 (EVER).” September 27–30, 2017, Nice, France.
 9. Kadziauskienė A., Kuolienė K., Galgauskas S., Ašoklis R. “Changes in Choroidal Thickness after Intraocular Pressure Reduction following Trabeculectomy.” Poster. International conference “The 6th World Glaucoma Congress.” June 6–9, 2015, Hong Kong.

CURRICULUM VITAE

Personal information

Name: Aistė Kadziauskienė
Address: 35 Širvintų St., Vilnius, Lithuania.
Email: aistedam@gmail.com

Work experience

2008 – present Ophthalmologist at Vilnius University Hospital Santaros Klinikos.
2008 – 2013 Assistant at the Clinic of the Ear, Nose, Throat, and Eye Diseases, Faculty of Medicine, Vilnius University.

Education

2013 – present PhD studies, Faculty of Medicine of Vilnius University.
2004 – 2008 Ophthalmology Residency, Faculty of Medicine of Vilnius University.
2003 – 2004 Internship, Faculty of Medicine of Vilnius University.
2000 – 2001 Medical studies, University of Eastern Finland.
1997 – 2003 Medical studies, Faculty of Medicine of Vilnius University. Graduation *Cum laude*.
1994 – 1997 Vilnius Lyceum of Natural and Technical Sciences.

Main publications

1. Kadziauskienė A, Jašinskienė E, Ašoklis R, Lesinskas E, Rekašius T, Chua J, Cheng CY, Mari JM, Girard MJA, Schmetterer L. Long-Term shape, curvature, and depth changes of the lamina cribrosa after trabeculectomy. *Ophthalmology*. 2018 Nov;125(11):1729–1740.
2. Kadziauskienė A, Kuolienė K, Ašoklis R, Lesinskas E, Schmetterer L. Changes in choroidal thickness after intraocular pressure reduction following trabeculectomy. *Acta Ophthalmologica*. 2016 Sep;94(6):586–91.
3. Kadziauskienė A, Strelkauskaitė E, Mockevičiūtė E, Ašoklis R, Lesinskas E, Schmetterer L. Changes in macular thickness after trabeculectomy with or without adjunctive 5-fluorouracil. *Acta Medica Lituanica*. 2017;24(2):93–100.
4. Ašoklis R, Kadziauskienė A, Paulavičienė R, Petroška D, Laurinavičius A. Quantitative histopathological assessment of

ocular surface squamous neoplasia using digital image analysis. *Oncology Letters*. 2014 Oct;8(4):1482–1486.

5. Ašoklis R, Damijonaitytė (Kadziauskienė) A, Butkienė L, Makselis A, Petroška D, Pajaujįs M, Juodkaitė G. Ocular surface reconstruction using amniotic membrane following excision of conjunctival and limbal tumors. *European Journal of Ophthalmology*. 2011 Sep-Oct; 21(5):552–8.

Membership in medical organizations

2014 – present Lithuanian Glaucoma Society
2008 – present Lithuanian Ophthalmology Society
2010; 2014 – 2017 European Association for Vision and Eye Research

Awards, scholarships

2016 Research Council of Lithuania, scholarship for academic achievements
2008 The Association for Research and Vision in Ophthalmology, “Developing Country Eye Researcher Fellowship.”
2006 European Board of Ophthalmology, Grant for a Residency Exchange.
2000 ERASMUS scholarship.
1999, 2000, 2001 D. & I. Valauskų award for academic achievements.

Languages

Lithuanian, English, Russian, basics of French and German.

ACKNOWLEDGEMENT

I would like to thank the many people I have worked with and learned from for their contributions to this research:

Prof. Dr. Eugenijus Lesinskas;
Assoc. Prof. Dr. Rimvydas Ašoklis;

My particular gratitude goes to **Prof. Dr. Leopold Schmetterer** for all his kind and insightful consultations, valuable comments, and constant support while planning and conducting the research, discussing results, and preparing publications.

Members of the Dissertation Defence Panel:
Prof. Dr. Janina Tutkuvienė, Assoc. Prof. Dr. Gerhard Garhöfer,
Prof. Dr. Ingrida Janulevičienė, Prof. Dr. Dalius Jatužis, and
Assoc. Prof. Dr. Giedrius Kalesnykas.

Assoc. Prof. Dr. Michael Girard;
Dr. Jacqueline Chua;
Assoc. Prof. Dr. Tomas Rekašius;

Ernesta Jašinskienė, Aušra Liveikienė, Sigita Speičienė, Eglė Drukteinienė, Aistė Augytė, Raminta Mikalauskienė, Jolita Ivančikienė, and the whole team of the Center of Eye Diseases at Vilnius University Hospital Santaros Klinikos.

My heartfelt thanks go to
my husband, Giedrius, and my children, Liepa, Rokas, and
Martynas for their supportive love.

NOTES

Vilnius University Press
Saulėtekio ave. 9, 10222 Vilnius
e-mail info@leidykla.vu.lt
Print run copies 40